ECF-100BC5-16-0028
Revision 0

Evaluation of Leaching Characteristics of Hexavalent Chromium from Contaminated 100-BC Sediments at Hanford Site to Estimate Time Dependent Mass flux For Fate and Transport Modeling

Prepared for the U.S. Department of Energy
Assistant Secretary for Environmental Management

Contractor for the U.S. Department of Energy
under Contract DE-AC06-08RL14788

P.O. Box 1600
Richland, Washington 99352

Approved for Public Release;
Further Dissemination Unlimited

ECF-100BC5-16-0028
Revision 0

Evaluation of Leaching Characteristics of Hexavalent Chromium from Contaminated 100-BC Sediments at Hanford Site to Estimate Time Dependent Mass flux For Fate and Transport Modeling

Document Type: ENV Program/Project: EP&SP

S. Mehta
CH2M HILL Plateau Remediation Company

Date Published
October 2016

Prepared for the U.S. Department of Energy
Assistant Secretary for Environmental Management

Contractor for the U.S. Department of Energy
under Contract DE-AC06-08RL14788

P.O. Box 1600
Richland, Washington 99352

APPROVED
By Lana Perry at 3:27 pm, Oct 19, 2016

Release Approval Date

Approved for Public Release;
Further Dissemination Unlimited

TRADEMARK DISCLAIMER

Reference herein to any specific commercial product, process, or service by tradename, trademark, manufacturer, or otherwise, does not necessarily constitute or imply its endorsement, recommendation, or favoring by the United States Government or any agency thereof or its contractors or subcontractors.

This report has been reproduced from the best available copy.

Printed in the United States of America

ENVIRONMENTAL CALCULATION COVER PAGE

Section 1: Completed by the Responsible Manager

Project: 100-BC Remedial Investigation/Feasibility Study

Date: 03/16/2016

Calculation Title & Description: Evaluation of Leaching Characteristics of Hexavalent Chromium from Contaminated 100-BC Sediments at Hanford Site to Estimate Time Dependent Mass flux For Fate and Transport Modeling

RELEASE / ISSUE

DATE: Oct 19, 2016 HANFORD RELEASE

Section 2: Completed by Preparer

Calculation No.: ECF-100BC5-16-0028 **Revision No.:** 0

Revision History

Revision No.	Description	Date	Affected Pages ADD ROW
0	Initial issue		All

Section 3: Completed by the Responsible Manager

Document Control:

Is the document intended to be controlled within the Document Management Control System (DMCS)? ☒ Yes ☐ No

Does document contain scientific and technical information intended for public use? ☒ Yes ☐ No

Does document contain controlled-use information? ☐ Yes ☒ No

Section 4: Document Review & Approval

	Name /Position	Signature	Date
Preparer:	S Mehta/Senior Scientist CHPRC		3/16/2016
Checker:	U. Zaher/Environmental Engineer		3/17 2016
Senior Reviewer:	G Ruskauff/Pr Hydrogeologist INTERA		3/17/16
Responsible Manager:	AH Aly / Risk & Model Integr CHPRC		3/17/16

Section 5: Applicable if calculation is a risk assessment or uses an environmental model

PRIOR TO INITIATING MODELING:

Required training for modelers completed:

	Name /Position	Signature	Date
Integration Lead	WE Nichols / Model Team Ldr CHPRC		16 MAR 2016

Safety Software Approved:

	Name /Position	Signature	Date
Integration Lead	WE Nichols / Model Team Ldr CHPRC		16 MAR 2016

CALCULATION APPROVED:

	Name /Position	Signature	Date
Risk/Modeling Integration Manager:	AH Aly / Risk & Model Integr CHPRC		3/17/16

Contents

1 Purpose **1**

2 Source Term Conceptual Model **2**

3 Methodology **4**

4 Assumptions and Inputs **7**

5 Software Applications **8**

6 Calculation **8**

7 Results **27**

8 Conclusions **32**

9 References **32**

Appendices

A Finite Difference Approximation ..... **A-i**

B MATLAB® Input File for Column 3 Kinetic Sorption Model Calculation ..... **B-i**

Figures

Figure 1. Location of the 100-BC Area Relative to the Hanford Site (Shown in Red Box) 1

Figure 2. Major Structures Used to Store and Dispose Reactor Coolant Waters at the 100-BC Area 2

Figure 3. Location of Cr(VI) Concentration in the Soil Samples Taken Prior To, During, and Post-Remediation 3

Figure 4. Conceptualization of Zone of Residual Contamination in the Vadose Zone Including the PRZ Resulting from Reaction of Acidic Sodium Dichromate Solutions with the Host Rock During Past Surface Discharges 4

Figure 5. Chromium Sampling Sites in the 100-BC Area 5

Figure 6. Leaching Profiles of Four Contaminated Sediments Collected from the 100-BC Area. 6

Figure 7. Rate of Cr(VI) Released Normalized to Initial Soil Concentration as a Function of Stop-Flow Event Duration 11

Figure 8. Cumulative Mass Fraction Released as a Function of Pore Volumes 12

Figure 9. Empirically Derived Desorption K_d for Various Column Tests as a Function of Pore Volumes Flushed 12

Figure 10. K_d Power Function Fit of K_d Values Derived from Data Until First Stop-Flow Event from All Columns 16

Figure 11. K_d Power Function Fit of all K_d Values Derived from All Data from All Columns 17

Figure 12. Comparison of Simulated to Observed Bromide Concentrations for Columns 3, 4, 5, and 6 18
Figure 13. Fitted Cr(VI) Concentrations Using Kinetic Sorption Model for Column 3 (Soil A1) 21
Figure 14. Fitted Cr(VI) Concentrations Using Kinetic Sorption Model for Column 4 (Soil A2) 21
Figure 15. Fitted Cr(VI) Concentrations Using Kinetic Sorption Model for Column 5 (Soil B1) 22
Figure 16. Fitted Cr(VI) Concentrations Using Kinetic Sorption Model for Column 6 (Soil D) 22
Figure 17. Fitted Cr(VI) Concentrations Using Equilibrium_All Model for Column 3 (Soil A1) 23
Figure 18. Fitted Cr(VI) Concentrations Using Equilibrium_All Model for Column 4 (Soil A2) 24
Figure 19. Fitted Cr(VI) Concentrations Using Equilibrium_All Model for Column 5 (Soil B1) 24
Figure 20. Fitted Cr(VI) Concentrations Using Equilibrium_All Model for Column 6 (Soil D) 25
Figure 21. Fitted Cr(VI) Concentrations Using Equilibrium_1stFlow Model for Column 3 (Soil A1) 25
Figure 22. Fitted Cr(VI) Concentrations Using Equilibrium_1stFlow Model for Column 4 (Soil A2) 26
Figure 23. Fitted Cr(VI) Concentrations Using Equilibrium_1stFlow Model for Column 5 (Soil B1) 26
Figure 24. Fitted Cr(VI) Concentrations Using Equilibrium_1stFlow Model for Column 6 (Soil D) 27
Figure 25. Mass Release Rates of Cr(VI) as a Function of Pore Volumes Based on the Kinetic and Equilibrium Sorption Models Normalized to Initial Soil Concentration and Darcy Flux 28
Figure 25. Mass Release Rates of Cr(VI) as a Function of Pore Volumes Based on the Kinetic and Equilibrium Sorption Models Normalized to Initial Soil Concentration and Darcy Flux 29
Figure 26. Regression Fit to Empirically Derived Desorption K_d Values Beyond 20 Pore Volumes 31
Figure 27. Leach Rate Constant Multiplier to Quantify the Declining Source Strength for Release of Cr(VI) 32

Tables

Table 1. Parameter Values for Column Leach Tests 7
Table 2. Rate of Cr(VI) Released Following Stop-Flow Events Based on Information Presented in PNNL-17674 9
Table 3. Initial Partition Coefficient Calculation Based on Initial Soil Concentration and Initial Dissolved Concentration for Modeling 14
Table 4. Input Parameters for Comparison to Bromide Transport 18
Table 5. Empirically Derived Reverse (Desorption) Reaction Rates of Cr(VI) from Stop-Flow-Event-Based Observations for Various Columns 19
Table 6. Fitted Reverse and Forward Reaction Rate Constants for Cr(VI) from Various Column Leach Tests 20

Terms

bgs	below ground surface
Ca	calcium
Cr	chromium
Cr(VI)	hexavalent chromium
ECF	environmental calculation file
Fe	iron
K_d	distribution coefficient
Mg	magnesium
Na	sodium
PVC	polyvinyl chloride
PRZ	periodically rewetted zone

This page intentionally left blank.

1 Purpose

The focus of this environmental calculation file (ECF) is to evaluate the leaching characteristics of hexavalent chromium (Cr(VI)) from the contaminated vadose zone sediments at the 100-BC Area (including the 100-BC-5 Operable Unit and surrounding region) of the Hanford Site and to develop transport parameters that can be used in predicting the long-term mass flux of Cr(VI) to the unconfined aquifer from contaminated sediments in the vadose zone and periodically rewetted zone (PRZ). Figure 1 shows the location of the 100-BC Area.

The primary objectives of the study are as follows:

1. Estimate time-dependent mass flux of hexavalent chromium [Cr(VI)] based on results of column leaching tests conducted on contaminated sediments collected from the 100-BC Area.

2. Develop scale-dependent desorption parameters that can be applied in a fate and transport model at the scale of the 100-BC Area. The parameters should be based on an internally self-consistent data set derived from leaching behavior of sediments that are representative of contaminated sediments in the 100-BC Area.

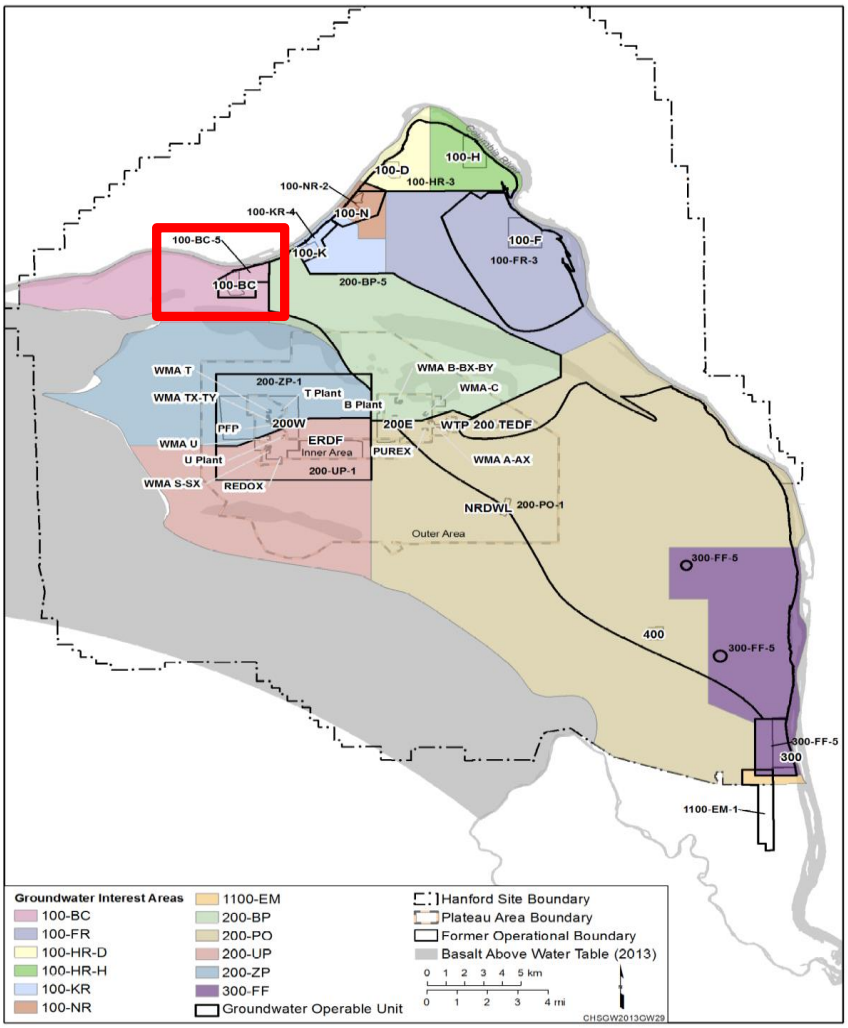

Figure 1. Location of the 100-BC Area Relative to the Hanford Site (Shown in Red Box)

2 Background: Source Term Conceptual Model

Cr(VI) occurs as a common contaminant in the vadose zone and groundwater in and around reactor operational areas along the Columbia River within the 100 Area of the Hanford Site. During reactor operations, sodium dichromate ($Na_2Cr_2O_7.2H_2O$) was mixed with reactor cooling water as a corrosion inhibitor. Historical records indicate that after a single pass through the reactors the waters were discharged into retention basins and allowed to infiltrate through the vadose zone into the underlying aquifer. Numerous spills of concentrated sodium dichromate solutions were also reported at various locations where salt solutions were mixed with river water before passing through the reactors.

The major structures that created, used, and disposed of reactor coolant at the 100-BC Area are shown in Figure 2. River water was pumped and stored in the 182-B Reservoir prior to transfer to 183-B and 183-C. At 183-B and 183-C, Columbia River water was purified and transferred to 190-B and 190-C, respectively, where sodium dichromate was added. Concentrated sodium dichromate starting materials, first as solids (until the mid-1950s at the 105-C Reactor and around 1960 at the 105-B Reactor) and then solutions, were stored at 190-B and 190-C and added to the purified Columbia River water to make reactor coolant. A loss of the highly concentrated sodium dichromate solution occurred around the storage tank at 183-C.

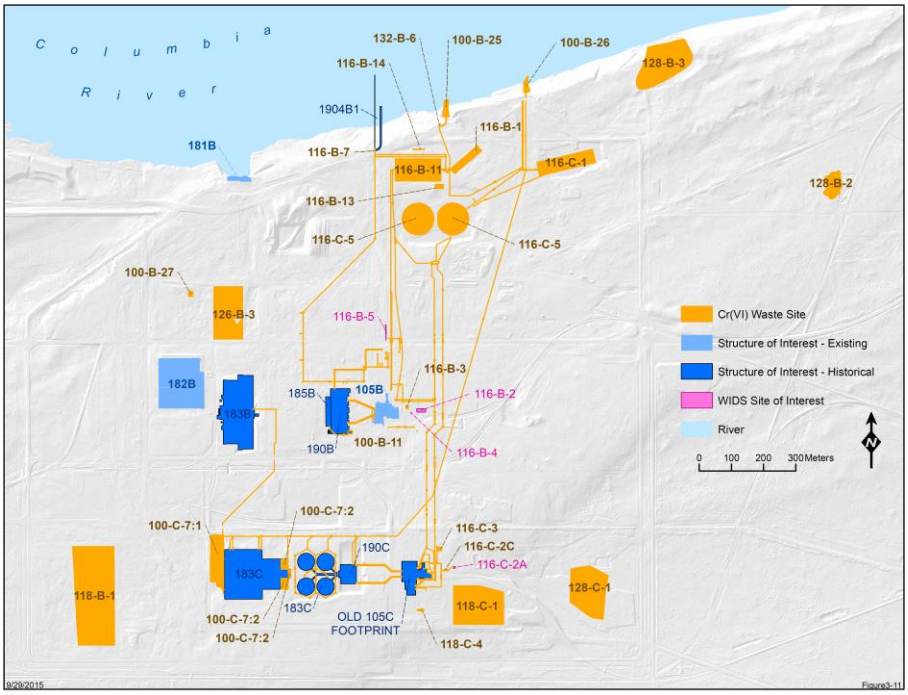

Figure 2. Major Structures Used to Store and Dispose Reactor Coolant Waters at the 100-BC Area

The reactor coolant was then routed through the 105-B and 105-C Reactors and piped to either the 116-B-11 or 116-C-5 Retention Basin. From these facilities, most of the coolant was then discharged to the river through three outfalls. Because of intermittent overflow of the retention basins or decisions to sequester specific coolant volumes contaminated by exposure to ruptured fuel elements, reactor coolant was also routed to the 116-B-1 and 116-C-1 Trenches. An additional discharge event occurred during early operations (1946) in which highly contaminated fuel storage basin water was discharged to the 116-B-2 Trench. Leaks were ubiquitous in pipelines and the retention basins. However, the fraction of

discharged volume that entered the Columbia River versus leakage into the vadose zone through infrastructure leaks is not known.

Figure 3 presents the Cr(VI) concentrations in soil reported prior to, during, and post-excavation of the various waste sites in the 100-BC Area (ECF-100BC5-15-0118, *Initial Chromium Concentration Development to Support Fate and Transport Modeling for Remedial Investigation/Feasibility Study of the 100-BC Operable Units*). It also includes the concentrations from the various boreholes. Figure 3 is intended to simply provide an overview of areal distribution of contamination prior to any remediation or soil removal activities; therefore, sample depth information is not presented. Additional details are presented in ECF-100BC5-15-0118.

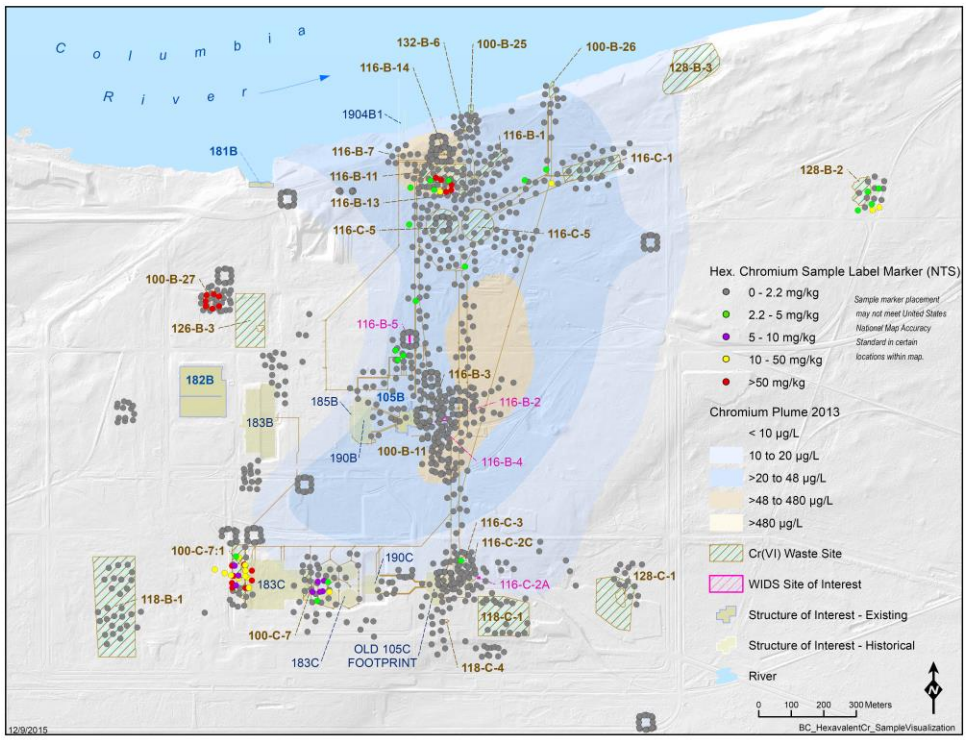

Note: The depth information is not presented in this figure.

Figure 3. Location of Cr(VI) Concentration in the Soil Samples Taken Prior To, During, and Post-Remediation

While the exact acidity of Hanford Site chromate stock solutions is not well known, a 10% $Na_2Cr_2O_7$ solution (0.82 mol/L Cr) has a pH of 3.5, and a 70% $Na_2Cr_2O_7$ solution (8.96 mol/L Cr) will be lower (~1.5 to 2) (PNNL-17674, *Geochemical Characterization of Chromate Contamination in the 100 Area Vadose Zone at the Hanford Site*). Acidic solutions containing Cr(VI) probably reacted with sediments while progressing through the vadose zone. This likely led to relatively fast dissolution of calcite and other carbonate phases present in the sediments, primarily at the mineral grain boundaries, leading to release of calcium (Ca) and slower dissolution of clay minerals leading to release of iron(II) (Fe(II)), sodium (Na), magnesium (Mg), aluminum, and silicon. As infiltrating plumes migrate through the vadose zone, the acid is eventually neutralized, resulting in the following:

- Precipitation of carbonates and co-precipitation of Ca-chromate

- Reaction with Fe(II) leading to partial reduction of Cr(VI) and co-precipitation with $Fe(OH)_3$ and $FeCO_3$.
- Association of Cr(VI) with Na and Mg salts

The degree of reaction within the vadose zone that could lead to dissolution and reprecipitation is dependent on the solution composition, the discharged volume, and the length of time over which discharges occurred. The reaction front would also be affected by the heterogeneity of the vadose zone sediments and their hydraulic properties. Although some lateral movement of the reaction front is likely, its primary path is vertically downward below the discharge location. Figure 4 shows a conceptualization of this, where the primary mineral reactions occur in the core of the vadose zone drainage pathway. With depth and due to heterogeneity and variable saturation, the reaction area increases and becomes extensive in the PRZ. Due to reaction and co-precipitation of chromium (Cr) with carbonates, iron oxyhydroxide, aluminum hydroxides, and Na and Mg salts, various Cr-bearing mineral phases of varying solubilities could be present in the vadose zone. As a result, the leaching characteristics can be variable both spatially and temporally as different Cr-bearing minerals/salts dissolve and control the release. The PRZ is likely to be the primary contributor of the contaminant mass to the water table since the sediments within the PRZ undergo more leaching than do sediments above the PRZ. In areas where the vadose zone along the drainage pathway is highly contaminated, the sediments above the PRZ likely continue to supply the contaminant mass to the PRZ leading to sustained groundwater plumes.

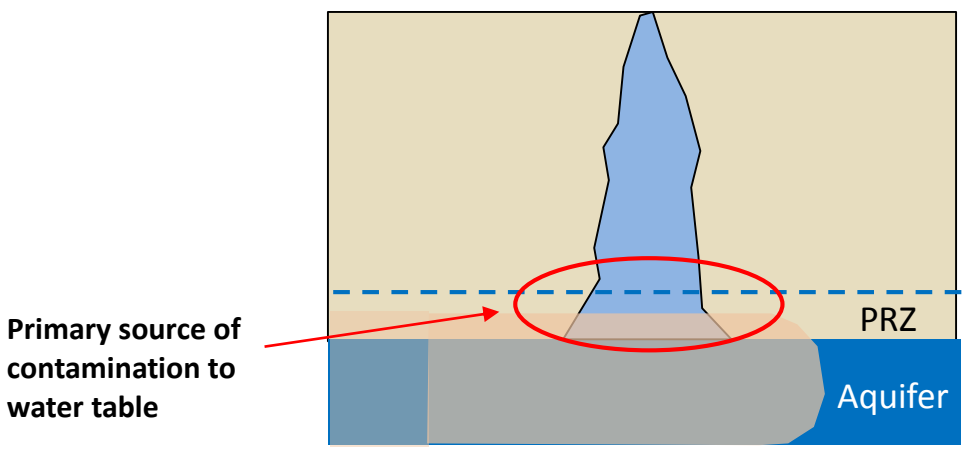

Figure 4. Conceptualization of Zone of Residual Contamination in the Vadose Zone Including the PRZ Resulting from Reaction of Acidic Sodium Dichromate Solutions with the Host Rock during Past Surface Discharges

3 Methodology

This study uses data from a series of flow-through column experiments designed to investigate Cr(VI) leaching under variable flow conditions from contaminated sediments in the 100-BC Area (PNNL-17674). As discussed in PNNL-17674, the vadose zone soil samples were collected from areas exposed to chromate contamination as shown in Figure 5. Location A samples were collected from the 100-C-7:1 site on the west side of the water treatment facility for the 100-C Reactor, north of the 183-C headhouse. This location included aboveground storage tanks for sodium dichromate solutions and sulfuric acid. Two samples (A1 and A2) were collected from an area of yellow stained soil located at the bottom of a pit approximately 3.7 m below ground surface (bgs). Location B samples were collected from the 100-B-27 unplanned release (surface spill) near railway tracks in the northeastern part of the

100-BC Area from depths of approximately 1.2 to 1.8 m bgs. Location D samples were collected from the 100-C-7 site on the north side of the 100-C Reactor water treatment facility from an area of contamination released during excavation of a sodium-dichromate pipeline in March 2005, where the pipeline solution had a Cr concentration of about 0.8 mol/L. Note that all samples were taken from shallow depths and from areas with high known contamination and therefore may not be completely representative of the contaminated sediments in the deeper part of the vadose zone. However, the results obtained from analyzing the leaching characteristics of these samples when compared with other leach studies conducted on samples collected elsewhere in the 100 Area (e.g., 100-D Area) could provide the range of variability in Cr(VI) leaching characteristics that can be expected in the vadose zone.

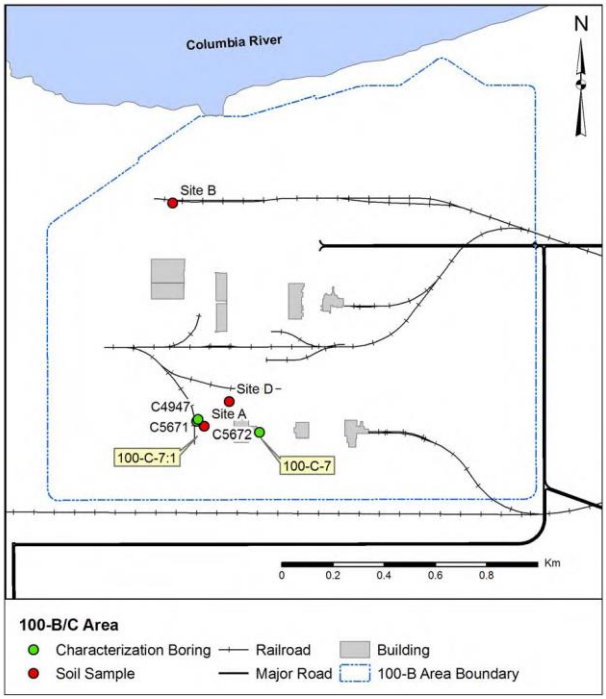

Figure 5. Chromium Sampling Sites in the 100-BC Area

Four detailed flow-through column leach tests were performed on sediment samples A1, A2, B, and D. The results are presented in Figure 6 in terms of dissolved Cr(VI) concentrations observed in the effluent sample collected at the end of the column as a function of pore volume (PNNL-17674). For the four soil samples, the corresponding column experiments are indexed as follows: Column 3 (for soil A1); Column 4 (for soil A2); Column 5 (for soil B1); and Column 6 (for soil D).

Polyvinyl chloride (PVC) columns (10.5 cm long and 2.5 cm inner diameter) were packed uniformly with the contaminated sediments. Uncontaminated groundwater was injected at the top of the column at a uniform rate. Contaminated effluent was collected at frequent intervals, and the effluent concentration was measured. Each experiment was ran with several stop-flow events (i.e., the influent is stopped and after a period of time flow is resumed). The concentration response during the stop-flow events provides evidence of the nonequilibrium sorption process. Samples of the effluent provide release concentrations. The soil types represent both aged and freshly contaminated sediments. The flow-through column experiments were also conducted by injecting a nonsorbing solute (bromide) in the influent. Evaluation of results of nonsorbing solute provided the transport properties such as average pore water velocity and dispersivity within the column, which was then used in the transport model to evaluate the desorption characteristics of Cr(VI).

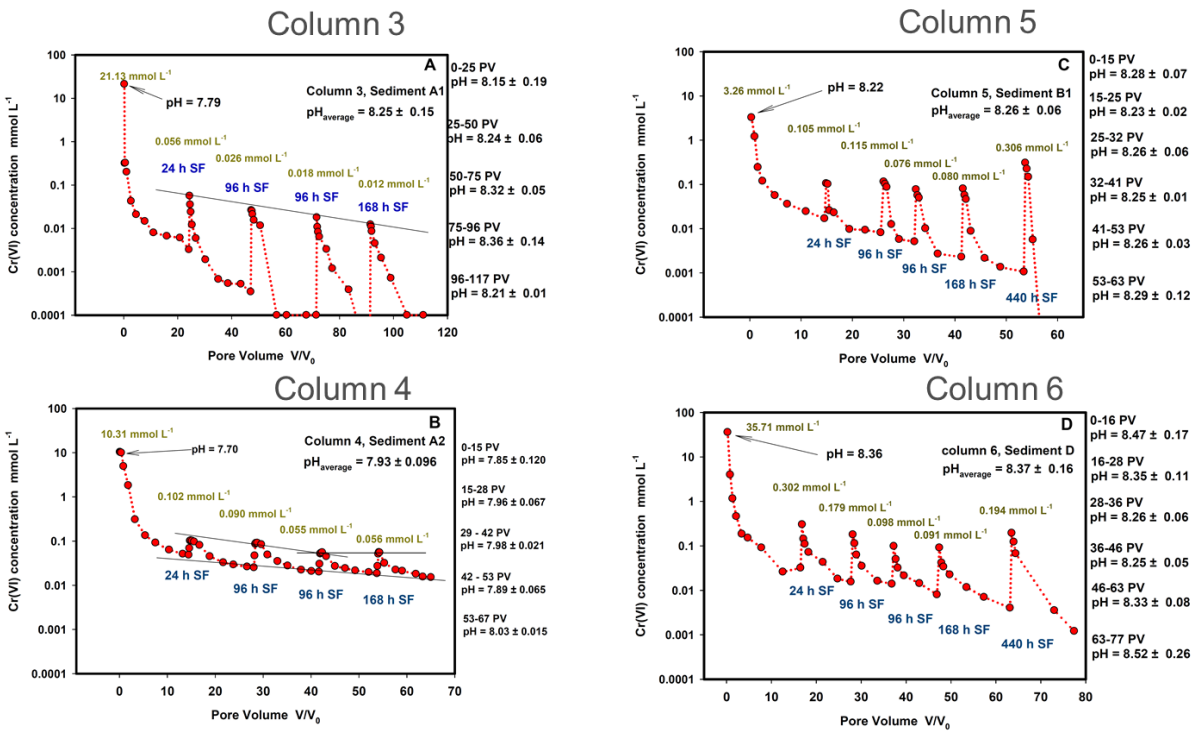

Note: Numerous stop-flow events were applied in each column experiment at different times during leaching.

Figure 6. Leaching Profiles of Four Contaminated Sediments Collected from the 100-BC Area.

In addition to the column tests, some <2 mm sized sediment fractions were analyzed for grain size distribution along with x-ray diffraction to estimate the silt and clay size fractions. The mass of easily separated silt and clay fractions varied in the sediments (sediment A1 = 18.99%, sediment A2 = 29.13 percent, sediment B = 7.04 percent, and sediment D = 20.84 percent). The main mineralogical components in all sediments were quartz, anorthite (feldspar), mica, clinochlore, vermiculite, and montmorillonite. In addition, x-ray microprobe and x-ray absorption near-edge structure techniques were used to measure the spatial distribution of Cr in the sediment samples. Element abundance maps for sediment A2 (old spill), sediment B (old spill), and sediment D (new spill) indicated that Cr was similarly dispersed around grain boundaries and also was found in the Cr-rich inclusions within the sediment matrix (Qafoku et al., 2009, *Pathways of Aqueous Cr(VI) Attenuation in a Slightly Alkaline Oxic Subsurface*). These measurements demonstrated that mixed valence Cr (Cr(VI) and Cr(III)) with variable Cr(VI)/Cr(III) ratios was present in the sediments. High-resolution imaging of the minerals associated with elevated Cr concentrations using scanning electron microscopy and energy dispersive spectroscopy indicated that Cr was associated with secondary mineral phases, such as aluminosilicates, Fe-rich aluminosilicate (most likely biotite and/or ferroan clinochlore), and/or Fe oxides (Qafoku et al., 2009). Secondary mineral domains within the sediment matrix may have hosted the Cr(VI) leaching-resistant fraction. Examination of Cr-rich areas found in two subsurface sediments collected from a borehole drilled in the same contaminated area as surface sediment D revealed that Cr was associated with magnetite and occurred as discrete $BaCrO_4$ particles.

The sediment characterization data clearly demonstrated that Cr(VI) reduction was neither significant nor complete in the sediments exposed to concentrated Cr waste liquids. Qafoku et al. (2009) note that there could be several reasons for partial Cr(VI) reduction, such as (1) reductants are not present in sufficient amount in the sediments to reduce available Cr(VI), and (2) the presence of nonconductive coatings (e.g., calcium carbonate or oxide coatings) on the surfaces of Fe(II)-bearing minerals and the creation of

passive Cr(III) layer on the surfaces of Fe(II)-bearing minerals may have led to reduced electron donor capacity or electron flow from the reductant to chromate.

This study develops a single-site kinetic sorption-desorption model that describes the contaminant transport consistent with the level of understanding of the underlying surface complexation processes and dissolution of mineral phases that control release of Cr(VI). Since these processes are complex and mechanistic models are lacking, a single-site kinetic sorption model provides a lumped parameter that provides good approximation to the empirical observations. Estimates of the kinetic sorption reaction rates are obtained by history matching the experimental data using a numerical model by applying boundary conditions that are consistent with the experimental setup. The numerical model is also used to match the nonsorbing bromide data, which provides a verification of the transport parameters.

An alternate release model based on equilibrium sorption-desorption parameters is also developed. The equilibrium sorption-desorption (K_d) model uses an empirical time-dependent partition coefficient determined from information extracted from the experimental results. The partition coefficient is represented as a function of the pore volumes of water through the column. Two different partition coefficient models are considered: one is based on simultaneous fitting of effluent data from all the columns to obtain desorption K_d as a function of pore volume, and the other is based on fitting the data until the first stop-flow event occurs for all the columns.

The results from fitting the data to the kinetic sorption and equilibrium sorption models are used to calculate mass release rates. The mass release rates are normalized with respect to the initial Cr soil concentration so that these rates can be applied to other locations where only Cr soil concentration is known, such as in the PRZ, aquifer, and vadose zone above the PRZ.

4 Assumptions and Inputs

Parameter values representing the four column experiments are shown in Table 1. Information required to simulate the leaching response was obtained from Table 3.2 of PNNL-17674 and includes the pore volume, water content, soil bulk density, injection rate, Darcy flux, and dispersion coefficient. The remaining parameters are computed from the given information. The bulk volume is the pore volume divided by the water content. The column cross-section area is the injection rate divided by the Darcy flux. The column length is the bulk volume divided by the area. These physical parameters are common to all subsequent calculation models. While conducting the column tests, the flow was stopped for variable time periods and then restarted. For each stop-flow event the initial concentration (prior to the stop-flow event) and final concentration (following resumption of flow) of the effluent was recorded (Table 2) along with other information about the experimental conditions (PNNL-17674).

Table 1. Parameter Values for Column Leach Tests

Parameter	Column 3 Soil A1	Column 4 Soil A2	Column 5 Soil B1	Column 6 Soil D
Pore volume (cm^3)	19.79	20.89	19.19	19.70
Water content	0.37	0.41	0.38	0.37
Soil bulk density (g/cm^3)	1.68	1.57	1.65	1.66
Injection rate (cm^3/hr)	20.0	11.8	11.6	14.9
Darcy flux (cm/hr)	3.90	2.34	2.34	2.88

Table 1. Parameter Values for Column Leach Tests

Parameter	Column 3 Soil A1	Column 4 Soil A2	Column 5 Soil B1	Column 6 Soil D
Dispersion coefficient (cm^2/hr)	27.3	10.1	5.21	29.3
Bulk volume (cm^3)	53.49	50.95	50.50	53.24
Area (cm^2)	5.114	4.980	4.909	5.078
Diameter (cm)	10.46	10.23	10.29	10.49

Source: PNNL-17674, *Geochemical Characterization of Chromate Contamination in the 100 Area Vadose Zone at the Hanford Site.*

5 Software Applications

The kinetic and equilibrium sorption models were solved using MATLAB[1] R2011b 7.13.0.564 software. In this calculation, MATLAB was used analogously with a flat-file spreadsheet in which the calculation is wholly incorporated into this environmental calculation file (ECF), and where the calculations, mathematical formulas, and input data were verified by the technical review of this ECF. Appendix B provides details regarding the calculations for Column 3 using the single-site kinetic sorption model. The entire input file used in the MATLAB is documented in Appendix B and verified by comparing to the mathematical formulation presented in Appendix A. Since the input file for other three columns (Columns 4, 5, and 6) is similar to that for Column 3, it is verified by comparing the files and noting the differences in input conditions.

Normalized release rates are calculated within Microsoft®[2] Excel®[3], which was also used as a flat-file spreadsheet in which the calculation is wholly incorporated into this ECF, and where the calculations, mathematical formulas, and input data were verified by the technical review of this ECF.

6 Calculation

From information presented in Table 2, the rate of Cr(VI) release at the resumption of a stop-flow event can be estimated. This release rate is divided by the initial Cr(VI) soil concentration to estimate the normalized release rate that can be then applied to any other soil concentration of Cr(VI). The results of the normalized release rates are presented as a function of stop-flow duration but converted to an equivalent normalized release per day as shown in Figure 7. The results indicate that the normalized release rates vary by over an order of magnitude and generally reduce with increased duration of the stop-flow event, which indicates that the mass release from desorption (and mineral-phase dissolution) into the pore water decreases with increasing stop-flow duration. Within the PRZ, due to daily fluctuations of the river stage, the duration of stop-flow events (rewetting cycles) is likely less than 24 hours. Therefore, the release rates based on a 24-hour stop-flow event are, in general, more representative of the PRZ. The normalized Cr(VI) release rates following the 24-hour stop-flow event range from 1×10^{-4} to 6×10^{-4} mg/day per mg/kg initial soil concentration.

1 MATLAB is a registered trademark of The Mathworks, Inc.

2 Microsoft is a registered trademark of Microsoft Corporation in the United States and in other countries.

3 Excel is a registered trademark of Microsoft Corporation in the United States and in other countries.

Table 2. Rate of Cr(VI) Released Following Stop-Flow Events Based on Information Presented in PNNL-17674

Stop-Flow Duration (hr)	Initial Cr(VI) (mg/L)	Final Cr(VI) (mg/L)	Conc. Difference (mg/L)	Conc. Difference (mmol/L)	Total Sediment mass (g)	Pore volume (mL)	Rate of Cr(VI) released (mmol/kg_soil/hr)	Log rate	Cumulative Pore volume	Initial Cr(VI) Soil Conc Alkaline Leach (mg_Cr/kg_soil)	Rate of Cr(VI) released (mg/kg_soil/hr)
Column 3											
24	0.168	2.926	2.758	0.0530	90.31	19.8	4.85E-04	-3.31	25.7	102.6	2.52E-02
96	0.018	1.36	1.342	0.0258	90.31	19.8	5.89E-05	-4.23	49.6	102.6	3.06E-03
96	0.0001	0.931	0.9309	0.0179	90.31	19.8	4.09E-05	-4.39	75.5	102.6	2.13E-03
168	0.003	0.639	0.636	0.0122	90.31	19.8	1.60E-05	-4.80	96.5	102.6	8.30E-04
Column 4											
24	2.51	5.325	2.815	0.0541	79.195	20.9	5.95E-04	-3.23	14.4	350.2	3.10E-02
96	1.305	4.693	3.388	0.0652	79.195	20.9	1.79E-04	-3.75	28.1	350.2	9.31E-03
96	1.042	2.868	1.826	0.0351	79.195	20.9	9.65E-05	-4.02	41.6	350.2	5.02E-03
168	0.958	2.896	1.938	0.0373	79.195	20.9	5.85E-05	-4.23	53.7	350.2	3.04E-03
Column 5											
24	0.878	5.47	4.592	0.0883	83.74	19.2	8.44E-04	-3.07	14.6	520.1	4.39E-02
96	0.422	5.99	5.568	0.1071	83.74	19.2	2.56E-04	-3.59	25.5	520.1	1.33E-02
96	0.264	4.002	3.738	0.0719	83.74	19.2	1.72E-04	-3.77	32.1	520.1	8.93E-03
168	0.1186	4.152	4.0334	0.0776	83.74	19.2	1.06E-04	-3.98	41.2	520.1	5.50E-03
440	0.055	15.93	15.875	0.3053	83.74	19.2	1.59E-04	-3.80	53.4	520.1	8.27E-03

Table 2. Rate of Cr(VI) Released Following Stop-Flow Events Based on Information Presented in PNNL-17674

Stop-Flow Duration (hr)	Initial Cr(VI) (mg/L)	Final Cr(VI) (mg/L)	Conc. Difference (mg/L)	Conc. Difference (mmol/L)	Total Sediment mass (g)	Pore volume (mL)	Rate of Cr(VI) released (mmol/kg_soil/hr)	Log rate	Cumulative Pore volume	Initial Cr(VI) Soil Conc Alkaline Leach (mg_Cr/kg_soil)	Rate of Cr(VI) released (mg/kg_soil/hr)
Column 6											
24	1.66	15.69	14.03	0.2698	88.895	19.7	2.49E-03	-2.60	16.5	1042.3	1.30E-01
96	0.803	9.3198	8.5168	0.1638	88.895	19.7	3.78E-04	-3.42	27.7	1042.3	1.97E-02
96	0.7203	5.1038	4.3835	0.0843	88.895	19.7	1.95E-04	-3.71	36.8	1042.3	1.01E-02
168	0.4146	4.7172	4.3026	0.0827	88.895	19.7	1.09E-04	-3.96	46.9	1042.3	5.68E-03
440	0.2084	10.0817	9.8733	0.1899	88.895	19.7	9.56E-05	-4.02	63.1	1042.3	4.97E-03

Source: PNNL-17674, *Geochemical Characterization of Chromate Contamination in the 100 Area Vadose Zone at the Hanford Site.*

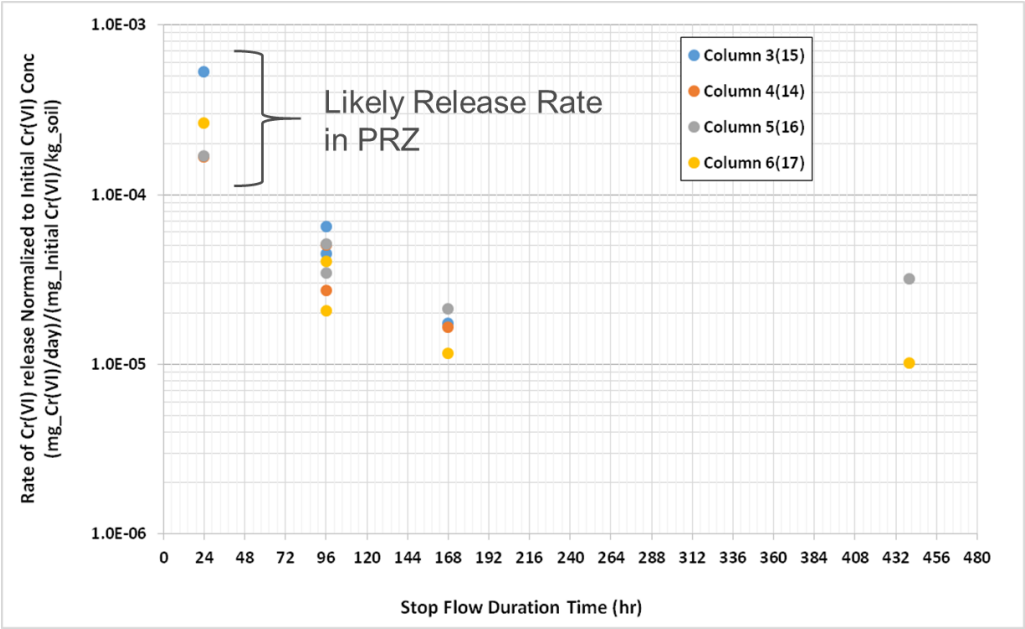

Figure 7. Rate of Cr(VI) Released Normalized to Initial Soil Concentration as a Function of Stop-Flow Event Duration

The column leach test results presented in Figure 6 were analyzed to estimate the cumulative mass released relative to the initial total Cr(VI) estimated based on soil concentration and soil mass within the column. The cumulative mass fraction released as a function of pore volumes is shown in Figure 8.

The results indicate that most of the leachable mass is released within about 20 pore volumes. After that the increase in mass release fraction is gradual, and by about 60 to 80 pore volumes almost all of the leachable mass has been released. The remaining mass is either not available for leaching or is being controlled by mineral phases with a very low rate of dissolution.

By tracking the released Cr(VI) mass as a function of pore volume and estimating the initial Cr(VI) mass available for potential release within the soil column (based on alkaline digestion), the mass remaining in the soil can be calculated at each pore volume. Using this information (sorbed concentration) along with the reported effluent concentration, a desorption K_d can be calculated as a function of pore volume. This empirically derived desorption K_d is calculated for each column and presented in Figure 9. The results indicate a generally increasing trend in K_d with increasing number of pore volumes, and therefore reflect dissolution of progressively less leachable mineral phase with which Cr is associated. Note that the y-axis is on the log scale. The intermittent declines in the desorption K_d result from the stop-flow event, where at resumption of flow, the dissolved concentrations are elevated, which leads to lowering of calculated K_d. However, the K_d values rise quickly and reach or exceed those calculated prior to the stop-flow event.

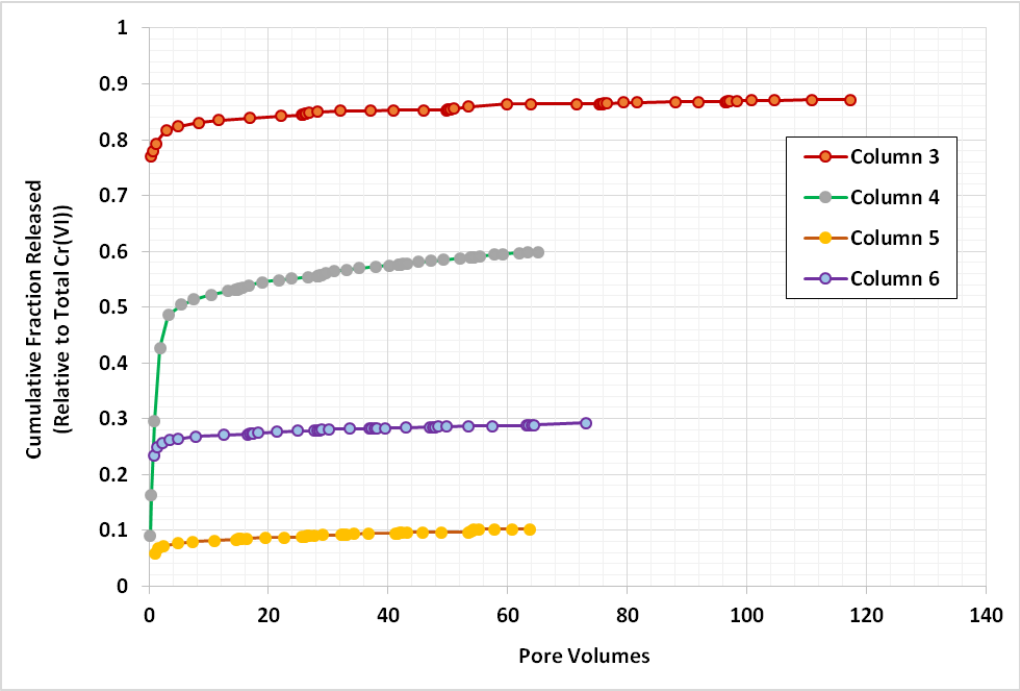

Figure 8. Cumulative Mass Fraction Released as a Function of Pore Volumes

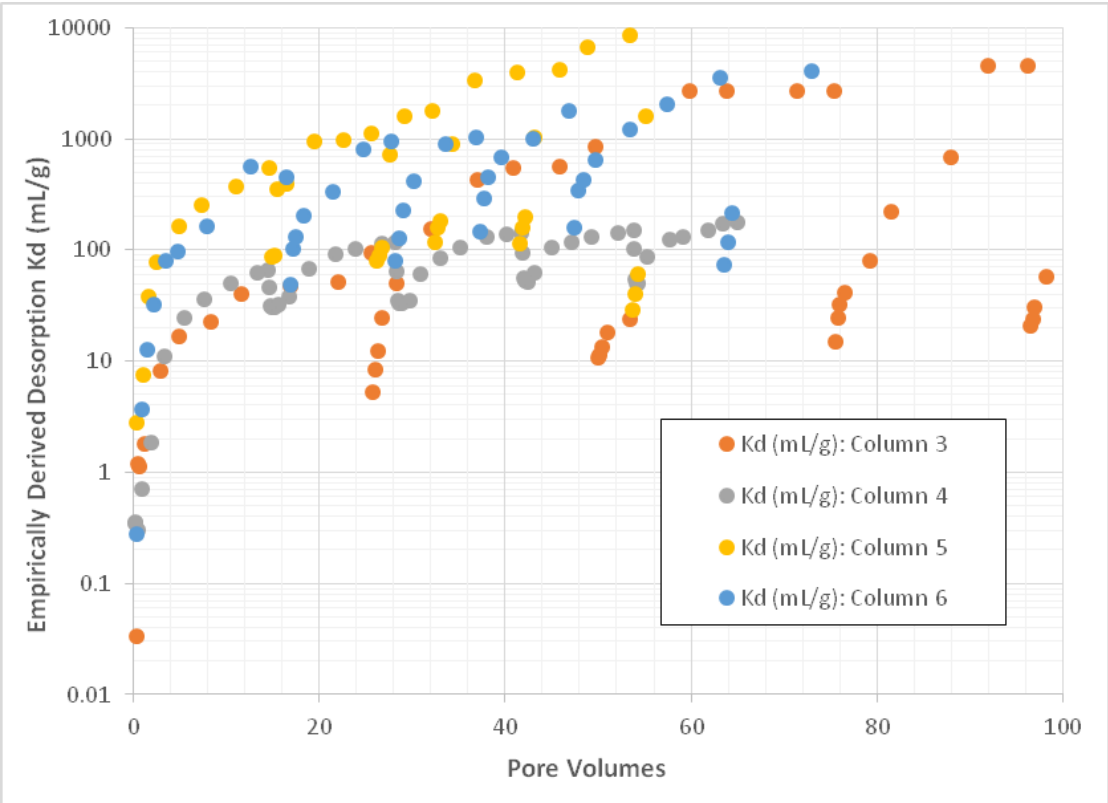

Figure 8. Empirically Derived Desorption K_d for Various Column Tests as a Function of Pore Volumes Flushed

The mathematical model for transport with kinetic sorption describes the advective/dispersive transport of a solute with both kinetic sorption and desorption in a saturated medium. The geometry is represented by a one-dimensional column. The mathematical model consists of mass balance equations for both the dissolved concentration and the solid concentration. The dissolved mass balance equation is shown in Equation 1:

$$\theta \frac{\partial C}{\partial t} = \theta D \frac{\partial^2 C}{\partial z^2} - v \frac{\partial C}{\partial z} - \rho_b \frac{\partial q}{\partial t} \qquad 0 < z < L \qquad \text{Equation 1}$$

The kinetic sorption equation is shown in Equation 2:

$$\rho_b \frac{\partial q}{\partial t} = \alpha_f \theta C - \alpha_r \rho_b q \qquad \text{Equation 2}$$

The forward and reverse reaction rates satisfy the relation:

$$\alpha_f = \alpha_r K_d \left(\frac{\rho_b}{\theta} \right) \qquad \text{Equation 3}$$

where:

C	=	dissolved concentration (mmol of Cr/cm^3 of water)
q	=	solid concentration (mmol of Cr/g of solid)
θ	=	water content, water volume/bulk volume (dimensionless)
v	=	Darcy velocity, water volume/area/time (cm/hr)
D	=	dispersion coefficient (cm^2/hr)
ρ_b	=	bulk density, matrix mass/bulk volume (g/cm^3)
α_f	=	forward reaction rate constant (hr^{-1})
α_r	=	reverse (desorption) reaction rate constant (hr^{-1})
K_d	=	equilibrium constant, volume water/soil mass (cm^3/g)

Equation 2 is expressed in terms of just the reverse reaction rate by substitution of Equation 3. The resulting kinetic sorption equation is shown in Equation 4:

$$\frac{\partial q}{\partial t} = \alpha_r K_d C - \alpha_r q \qquad \text{Equation 4}$$

The discharge or Darcy velocity is equal the water injection rate per unit area normal to flow. It is assumed there is no dispersion across the upper and lower boundaries. The influent has zero concentration; consequently, there is no advective transport at the upper boundary. The column contains Cr in both dissolved and solid states. Initially the dissolved and sorbed masses are assumed to be in equilibrium. This implies that the dissolved and solid concentrations are constant throughout the column.

At initial time the solid concentration is in equilibrium with the dissolved concentration if

$$\frac{\partial q}{\partial t}(z,0) = 0$$

which, from Equation 4, implies $q(z,0) = K_d C(z,0)$

The initial K_d value (at t = 0) is estimated based on Cr(VI) concentrations in the initial pore waters extracted from the sediments (based on centrifugation and extraction into water using a water-to-soil ratio of 3:1) and alkaline leach-based concentration of Cr(VI) in the soil (PNNL-17674). Table 3 presents the soil concentration estimate based on both water extraction and alkaline digestion (extraction) methods. The alkaline extraction results consistently showed higher levels of Cr(VI) than the water extraction and therefore represent the bounding estimate of the leachable mass of Cr(VI) over the long term (several pore volumes). The alkaline extraction results provided the best measurements of total Cr(VI) in the samples and are therefore used in the modeling calculations. The initial K_d value is based on initial soil concentration based on alkaline extraction.

Table 3. Initial Partition Coefficient Calculation Based on Initial Soil Concentration and Initial Dissolved Concentration for Modeling

Column-Soil	Initial Cr(VI) Soil Concentration (mg/kg) Based on Water Extraction	Initial Cr(VI) Soil Concentration (mg/kg) Based on Alkaline Extraction	Initial Dissolved Concentration in the Pore Water (mg/L)	Initial K_d (mL/g)*
Column 3: Soil A1	99.2	102.6	1612	0.06365
Column 4: Soil A2	117.2	350.2	437	0.8014
Column 5: Soil B1	339.7	520.1	4793	0.1085
Column 6: Soil D	810.4	1042.3	16846	0.06187

Source: PNNL-17674, *Geochemical Characterization of Chromate Contamination in the 100 Area Vadose Zone at the Hanford Site*.

* Based on initial soil concentration using alkaline extraction rather than water extraction.

The experimental results are presented as dissolved concentration as a function of cumulative water pore volumes. The relation between time and pore volumes is shown in Equation 5:

$$\Delta PVs = \frac{Q_{inj}\Delta t}{\theta V_{bulk}} \qquad \text{Equation 5}$$

where:

Q_{inj} = water injection rate (cm^3/hr)

Δt = time increment (hr)

V_{bulk} = column bulk volume (cm^3)

ΔPV = pore volume increment

During stop-flow events time is incremented while pore volume remains constant.

The mathematical model is approximated by a finite difference scheme. The details are presented in Appendix A and summarized here.

Consider a finite difference discretization of space and time. Denote the spatial cell index, i = 1, 2, …, Nz, where Nz is the number of grid cells. Let the time discretization be denoted $0 = t_0 < t_1 < t_2 < \ldots < t_{Nt}$ where Nt is the number of time steps. The discretization is fully implicit and uses approximations that are first order for time derivatives, first order with upstream weighting for advective transport, and second order for dispersive transport. The discretization for the ith cell and time step from t_n to t_{n+1} for the transport equation in tridiagonal form is shown in Equation 6:

$$-\left(\frac{\theta D}{\Delta z^2}+\frac{v}{\Delta z}\right)C_{i-1}^{n+1}+\left(\frac{2\theta D}{\Delta z^2}+\frac{v}{\Delta z}+\frac{\theta}{\Delta t}\right)C_i^{n+1}-\frac{\theta D}{\Delta z^2}C_{i+1}^{n+1}+\frac{\rho_b}{\Delta t}q_i^{n+1} = \frac{\theta}{\Delta t}C_i^n+\frac{\rho_b}{\Delta t}q_i^n \qquad \text{Equation 6}$$

and for the kinetic sorption equation

$$-\frac{\alpha_f\theta}{\rho_b}C_i^{n+1}+\left(\frac{1}{\Delta t}+\alpha_r\right)q_i^{n+1}=\frac{q_i^n}{\Delta t} \qquad \text{Equation 7}$$

This coupled system of equations uses known information at the beginning of the time step, C_i^n and q_i^n, to calculate the concentrations C_i^{n+1} and q_i^{n+1}

At the upper cell a no-flow condition is imposed for both dispersive and advective transport. At the lower boundary there is no dispersive transport. The advective mass transport at the lower boundary of the column, $i = Nz$, is computed as $Q_{inj}\Delta t C_{Nz}^{n+1}$ The effluent concentration reported is the concentration at grid block $i = Nz$.

An alternate Cr(VI) release model is developed based on an equilibrium sorption model using the desorption K_d (Figure 9), which varies as a function of the cumulative pore volume displacement. Under the conditions when the desorption kinetics are fast relative to the residence time of water (function of flow rate), the local equilibrium conditions would be reached that can be represented by using the desorption K_d model. Within the vadose zone and the PRZ where the pore water velocities are much lower than in the aquifer the establishment of local equilibrium is likely, and therefore the equilibrium sorption model may be a reasonable approximation for evaluating the long-term leach rate. Under equilibrium conditions, the column dissolved concentration is assumed to equal the effluent concentration, implying that the column acts as a well-mixed batch reactor with uniform concentration. With the initial mass in place, the dissolved mass, and the cumulative mass released, a mass balance calculation provides the solid mass or concentration.

The K_d data from all four columns from the initial start flow to the first stop-flow event are shown in Figure 10. The power function fit provides the relationship between K_d and the pore volumes. This approach is designated Equilibrium_1stFlow model. An alternative empirical partition coefficient fit is obtained by considering K_d data from all columns and for all column results. This is designated as Equilibrium_All model. The partition coefficient data and the power function fit for this model are shown in Figure 11 along with the fit derived from Equilibrium_1stFlow model. The partition coefficient approximation using just the first flow event-based fit results in a higher K_d, since the stop-flow events

result in lower K_d estimates. The results of these two alternative equilibrium models are reported as shown in Equations 8 and 9:

Equilibrium_1stFlow model:

$$K_d = 3.3621 * PV^{1.4749} \qquad \text{Equation 8}$$

Equilibrium_All model:

$$K_d = 4.1337 * PV^{1.0447} \qquad \text{Equation 9}$$

In order to implement the empirical partition coefficients given by Equations 8 and 9, it was necessary to include an additive threshold value when t = 0 or PV = 0. The partition function is then

$$K_d(PV) = K_d(0) + \alpha PV^{\beta} \qquad \text{Equation 10}$$

where the threshold value, $K_d(0)$, is the initial partition coefficient used for the kinetic sorption model that is taken from Table 3. The coefficients α and β are taken from coefficients presented in Equations 8 and 9 based on power function fit.

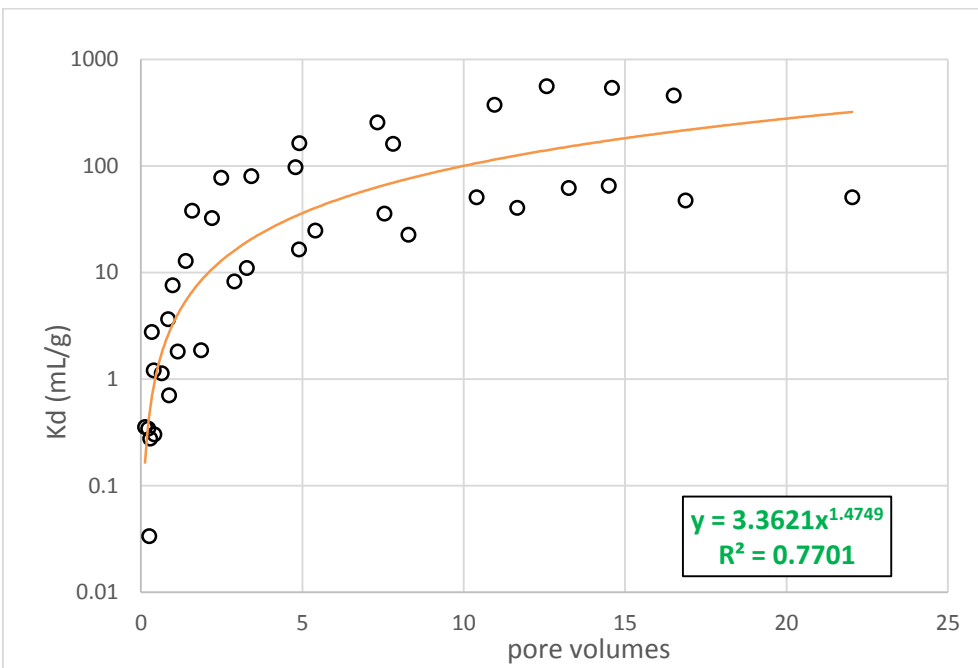

Figure 9. K_d Power Function Fit of K_d Values Derived from Data Until First Stop-Flow Event from All Columns

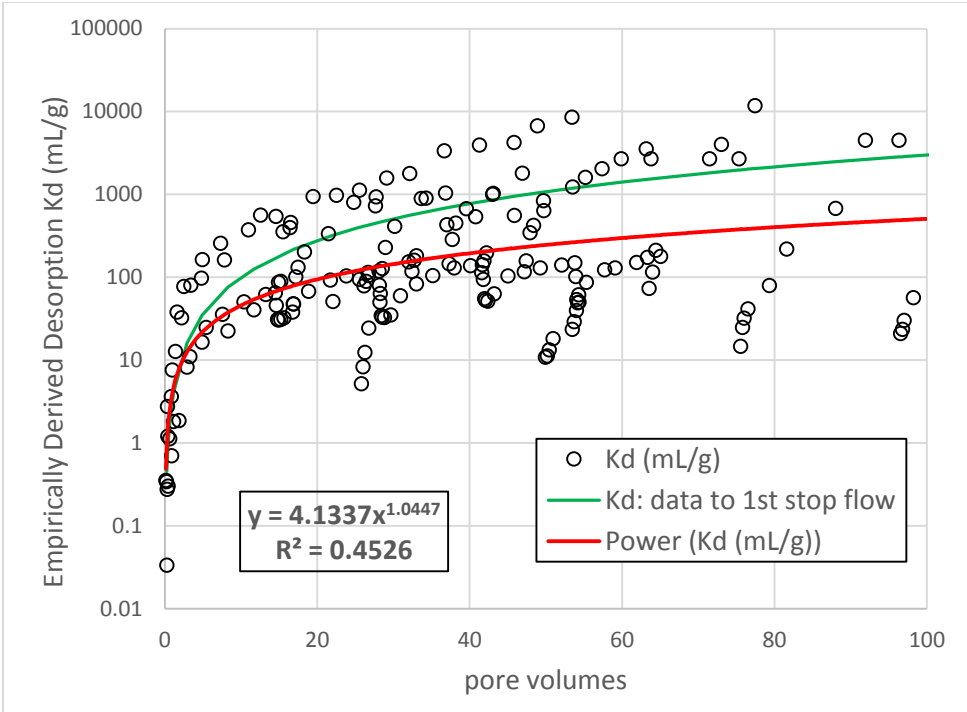

Figure 10. K_d Power Function Fit of all K_d Values Derived from All Data from All Columns

The transport equation with equilibrium sorption coefficient as a function of time is shown in Equation 11:

$$\theta \frac{\partial C}{\partial t} + \rho_b \frac{\partial}{\partial t}\left(K_d(t)C\right) = \theta D \frac{\partial^2 C}{\partial z^2} - v\frac{\partial C}{\partial z} \qquad \text{Equation 11}$$

The finite difference approximation in tridiagonal form is shown in Equation 12:

$$-\left(\frac{\theta D}{\Delta z^2} + \frac{v}{\Delta z}\right)C_{i-1}^{n+1} + \left(\frac{\theta}{\Delta t} + \frac{\rho_b K_d^{n+1}}{\Delta t} + \frac{2\theta D}{\Delta z^2} + \frac{v}{\Delta z}\right)C_i^{n+1} - \frac{\theta D}{\Delta z^2}C_{i+1}^{n+1} = \frac{\theta C_i^n}{\Delta t} + \frac{\rho_b K_d^n C_i^n}{\Delta t} \qquad \text{Equation 12}$$

All of the transport models report concentration as a function of pore volumes of water through the column, which is consistent with the representation of the laboratory data.

Experimental results for the four columns conducted by introducing nonsorbing bromide in the column are first evaluated. Comparing the model results to the observations for such a nonsorbing conservative species provides confidence in the model parameters, such as bulk water content (effective porosity), average flow rates, and longitudinal dispersivity. Input parameters for the bromide simulations based on available details about the experiment are shown in Table 4. Note that for Columns 3 and 5 the bromide concentration is present in the column prior to injection of clean water, leading to its displacement (flushing out). For Column 4 bromide is introduced as an influent (no initial concentration), whereas for Column 6 bromide is present in influent as well as present as initial concentration in Column 6.

Table 4. Input Parameters for Comparison to Bromide Transport

Parameters	Column 3 Soil A1	Column 4 Soil A2	Column 5 Soil B1	Column 6 Soil D
Column length (cm)	10.46	10.232	10.287	10.425
Column diameter (cm)	2.552	2.518	2.5	2.543
Water content	0.37	0.41	0.38	0.37
Dispersion (cm^2/hr)	27.3	10.1	5.21	29.3
Water injection rate (cm^3/hr)	19.98	11.76	11.64	14.88
Concentration injection stream (mg/cm^3)	0	0.13	0	0.03
Initial bromide concentration (mg/cm^3)	0.087	0	0.133	0.001

The simulation results and experimental observations of the bromide transport for the four soils are shown in Figure 12. A good agreement is observed that demonstrates that the input data and transport parameters are estimated and implemented correctly for a nonsorbing solute.

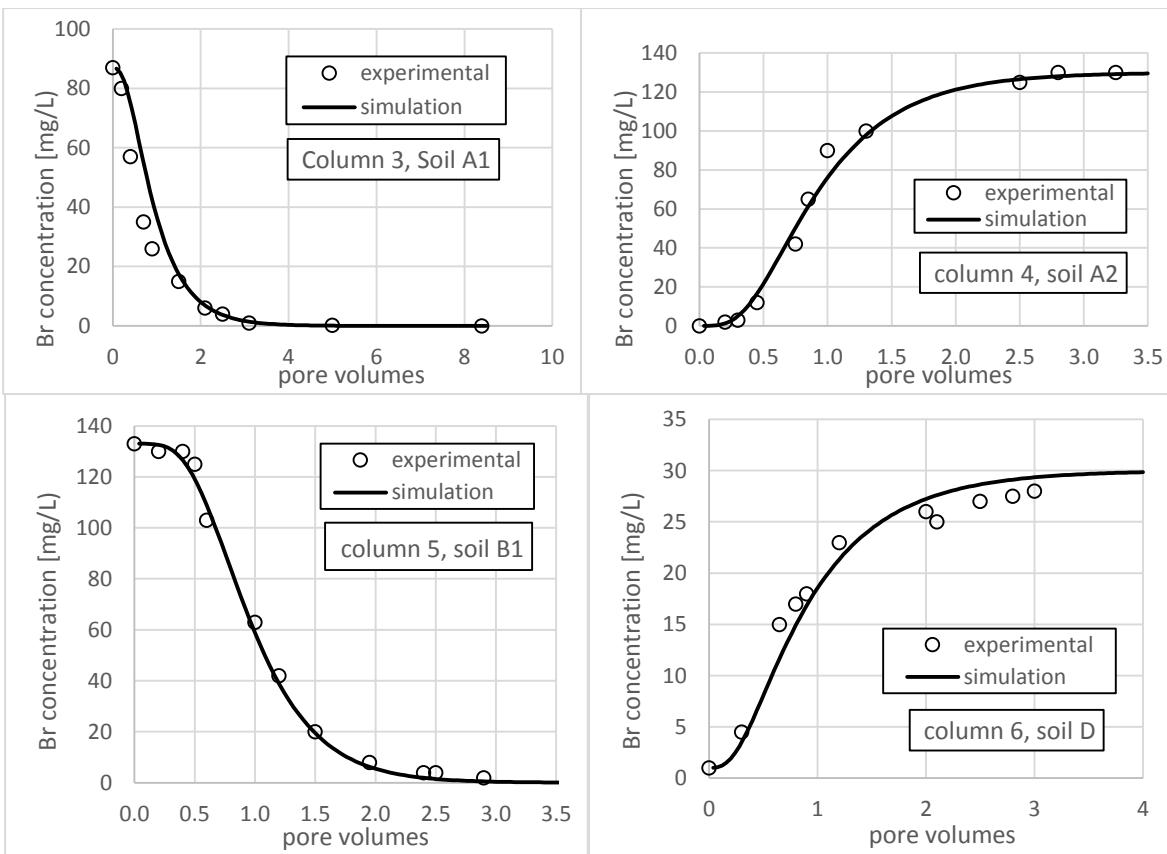

Figure 11. Comparison of Simulated to Observed Bromide Concentrations for Columns 3, 4, 5, and 6

Using the numerical implementation developed for modeling bromide transport but adding the kinetic sorption model, simulations were conducted to match the experimental results for Cr(VI) in the

column tests. This requires determining the value for reverse (desorption) reaction rate constant, α_r (see Equation 4), which best approximates the experimental effluent concentrations. The rate at which Cr(VI) is released during the stop-flow events is calculated in Table 2. From this the reverse reaction rate (desorption rate) constant can be estimated as shown in Table 5. The reverse (desorption) rate constant varies from 8×10^{-6} hr^{-1} to 3×10^{-4} hr^{-1} with the median value of about 2×10^{-5} hr^{-1}. This reverse reaction rate constant is chosen as an initial estimate for fitting the flow-through column results and varied within the range to get the best fit. Because the objective is to develop reaction rate parameters that can be applied under both static and flowing conditions, visual comparison of the fits was deemed sufficient. The forward reaction rate constant was derived from Equation 3. The final parameter values based on the fitting are summarized in Table 6 for all column tests evaluated. For starting the calculations, the initial solid concentrations, initial dissolved concentrations, and initial partition coefficient (K_d) are taken from Table 3.

Table 5. Empirically Derived Reverse (Desorption) Reaction Rates of Cr(VI) from Stop-Flow-Event-Based Observations for Various Columns

Stop-Flow Duration	Initial Cr(VI) Soil Concentration* Alkaline Leach (mg_Cr/kg_soil) [X]	Rate of Cr(VI) Released* (mg/kg_soil/hr) [Y]	Rate of Cr(VI) Released (1/hr) [Y]/[X]
Column 3			
24 hr	102.6 (Column 3: Soil A1)	2.52E-02	2.46E-04
96 hr		3.06E-03	2.99E-05
96 hr		2.13E-03	2.07E-05
168 hr		8.30E-04	8.09E-06
Column 4			
24 hr	350.2 (Column 4: Soil A2)	3.10E-02	8.84E-05
96 hr		9.31E-03	2.66E-05
96 hr		5.02E-03	1.43E-05
168 hr		3.04E-03	8.69E-06
Column 5			
24 hr	520.1 (Column 5: Soil B1)	4.39E-02	8.43E-05
96 hr		1.33E-02	2.56E-05
96 hr		8.93E-03	1.72E-05
168 hr		5.50E-03	1.06E-05
440 hr		8.27E-03	1.59E-05

Stop-Flow Duration	Initial Cr(VI) Soil Concentration* Alkaline Leach (mg_Cr/kg_soil) [X]	Rate of Cr(VI) Released* (mg/kg_soil/hr) [Y]	Rate of Cr(VI) Released (1/hr) [Y]/[X]
Column 6			
24 hr	1042.3 (Column 6: Soil D)	1.30E-01	1.24E-04
96 hr		1.97E-02	1.89E-05
96 hr		1.01E-02	9.71E-06
168 hr		5.68E-03	5.45E-06
440 hr		4.97E-03	4.77E-06

* From Table 2.

Table 6. Fitted Reverse and Forward Reaction Rate Constants for Cr(VI) from Various Column Leach Tests

Column	Reverse (Desorption) Reaction Rate Constant (1/hr)	Forward Reaction Rate Constant (1/hr)
Column 3: Soil A1	1×10^{-5}	2.8×10^{-6}
Column 4: Soil A2	6×10^{-4}	5.9×10^{-4}
Column 5: Soil B1	7×10^{-5}	2.1×10^{-4}
Column 6: Soil D	1×10^{-4}	2.1×10^{-5}

Figures 12 through 16 show the resulting concentration history match for Columns 3 through 6, respectively, compared to the observations. The emphasis is to match the observed values after several pore volumes have been flushed (typically greater than 20 pore volumes) to derive parameters that are applicable to predicting the long-term leachability of contaminated 100-BC Area sediments that likely have undergone several pore volume exchanges and where long-term release of Cr(VI) is controlled by slow dissolution of Cr-bearing mineral phases. There is less emphasis for fitting on early pore volume release characteristics as it typically results from flushing of highly dissolvable Cr salts precipitated in the pore spaces. The reverse (desorption) reaction rate constants vary from a minimum of 1×10^{-5} hr^{-1} to a maximum of 6×10^{-4} hr^{-1}.

As discussed earlier, an alternate Cr(VI) release model is developed based on equilibrium sorption model using the desorption K_d (Figures 10 and 11), which varies as a function of the cumulative pore volume displacement. Under the conditions when the desorption kinetics are fast relative to the residence time of water (function of flow rate), the local equilibrium conditions would be reached that can be represented by using the desorption K_d model. Within the vadose zone and the PRZ where the pore water velocities are much lower than in the aquifer the establishment of local equilibrium is likely, and therefore the equilibrium sorption model may be a reasonable approximation for evaluating the long-term leach rate.

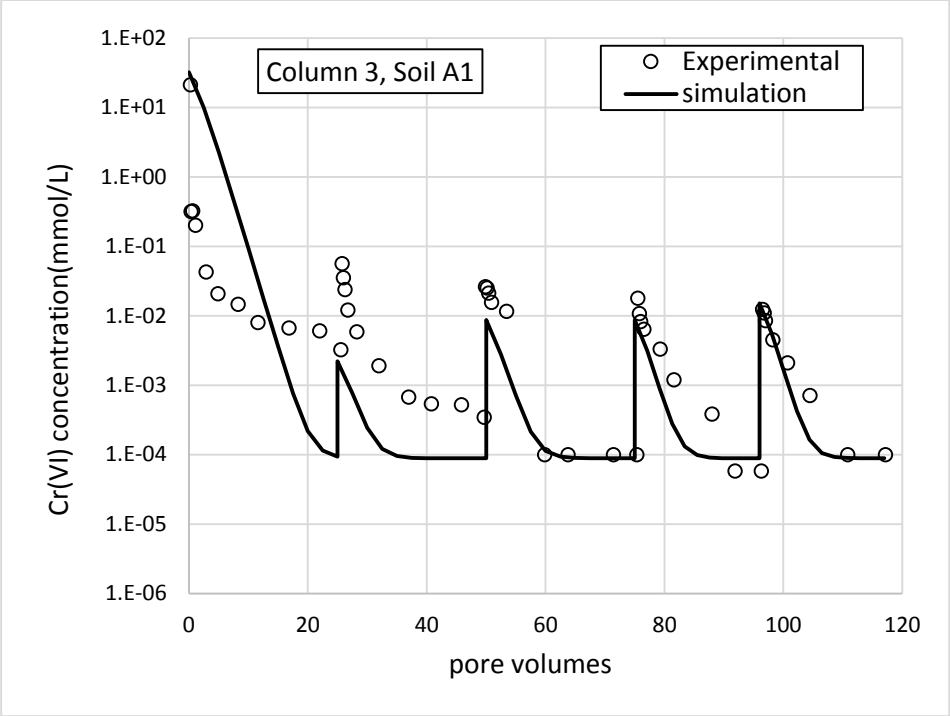

Figure 12. Fitted Cr(VI) Concentrations Using Kinetic Sorption Model for Column 3 (Soil A1)

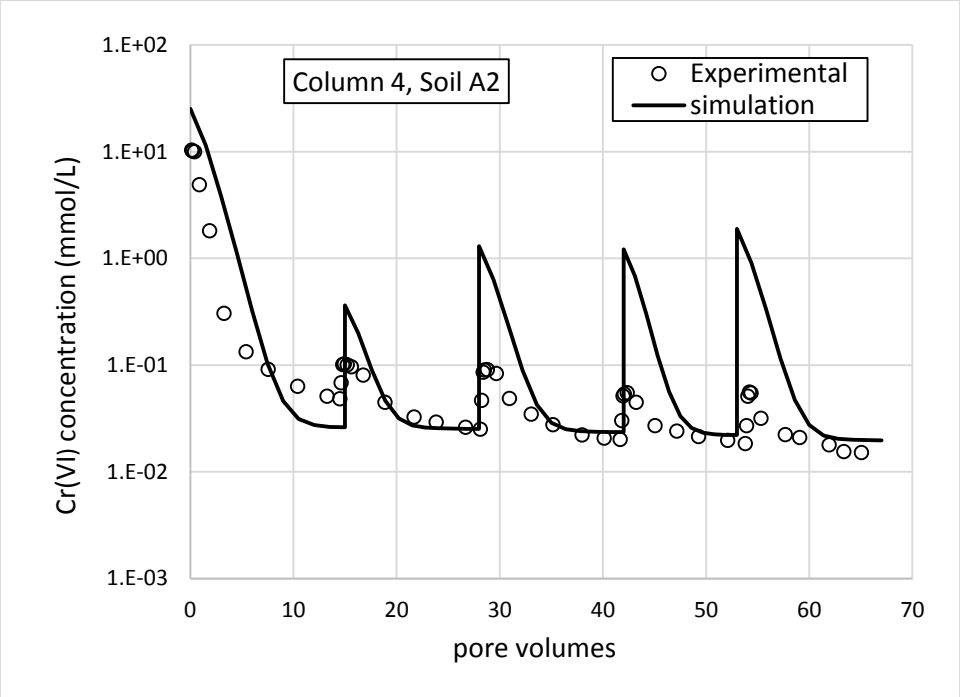

Figure 13. Fitted Cr(VI) Concentrations Using Kinetic Sorption Model for Column 4 (Soil A2)

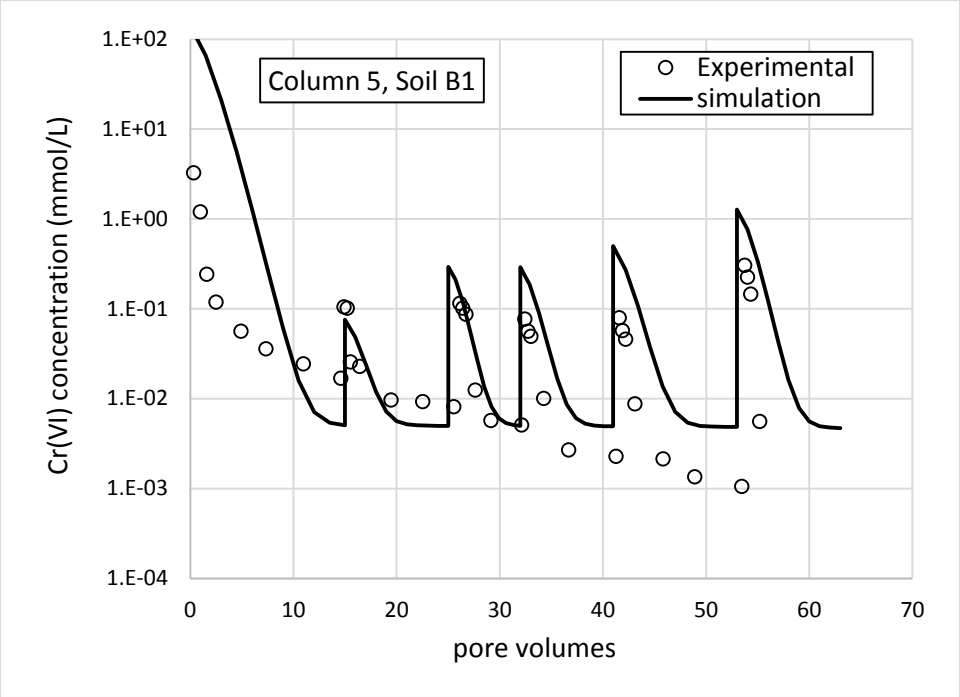

Figure 14. Fitted Cr(VI) Concentrations Using Kinetic Sorption Model for Column 5 (Soil B1)

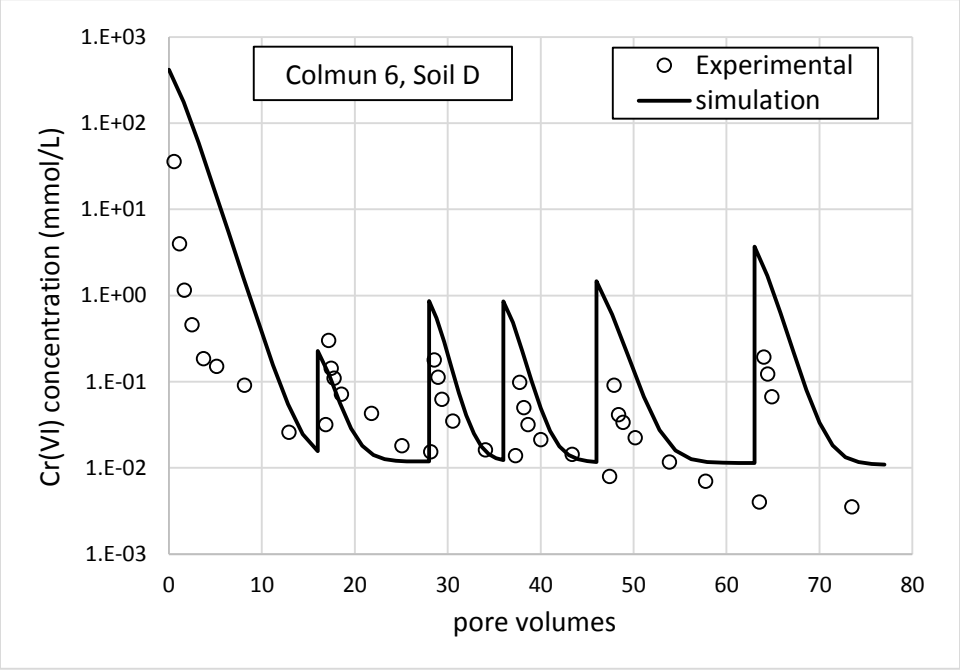

Figure 15. Fitted Cr(VI) Concentrations Using Kinetic Sorption Model for Column 6 (Soil D)

The equilibrium sorption model uses the same physical data, hydrologic data, soil data, and injection rates for each column. The results for the Equilibrium_All simulations (using Equation 9) are shown in Figures 17 through 20 for Columns 3 through 6, respectively. The results for the Equilibrium_1stFlow simulations (using Equation 8) are shown in Figures 21 through 24. For both the Equilibrium_All and the Equilibrium_1stFlow models, the simulated concentration results for Column 4 are a close fit to the

experimental effluent concentrations; but for Columns 3, 5, and 6, the simulated concentrations are slightly higher values than observed. One possible explanation is that the desorption kinetics for Column 4 are faster than for other columns and represent the natural variability expected in the field. The simulated fits are better when compared to the concentrations during and after resumption of the stop-flow events, indicating that equilibrium models provide a reasonable approximation of desorption behavior in vadose zone and PRZ.

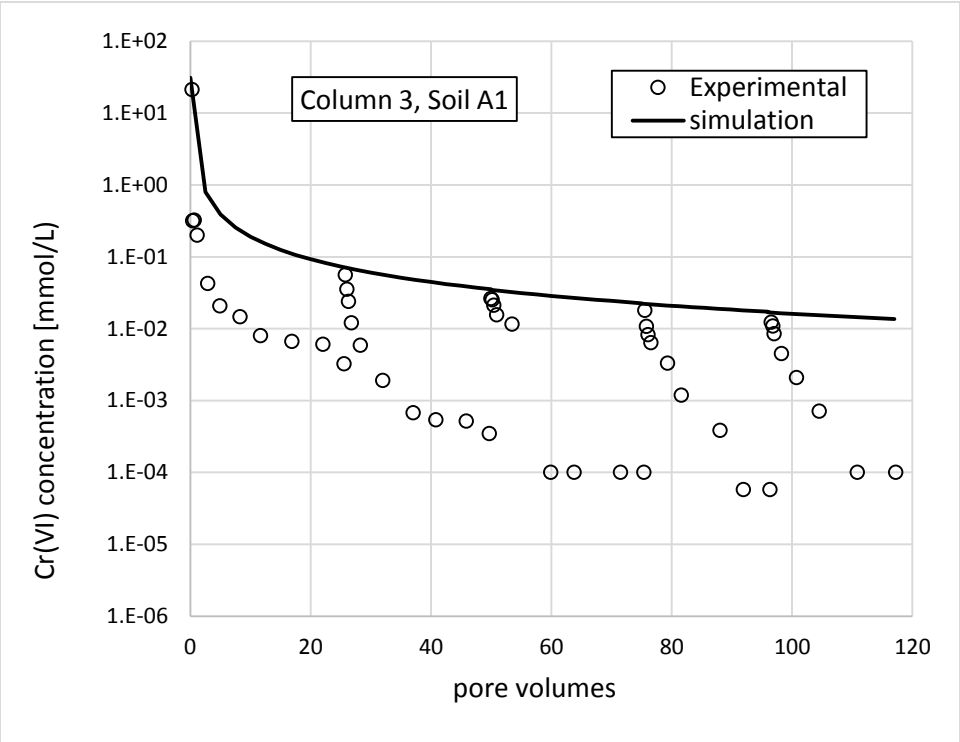

Figure 16. Fitted Cr(VI) Concentrations Using Equilibrium_All Model for Column 3 (Soil A1)

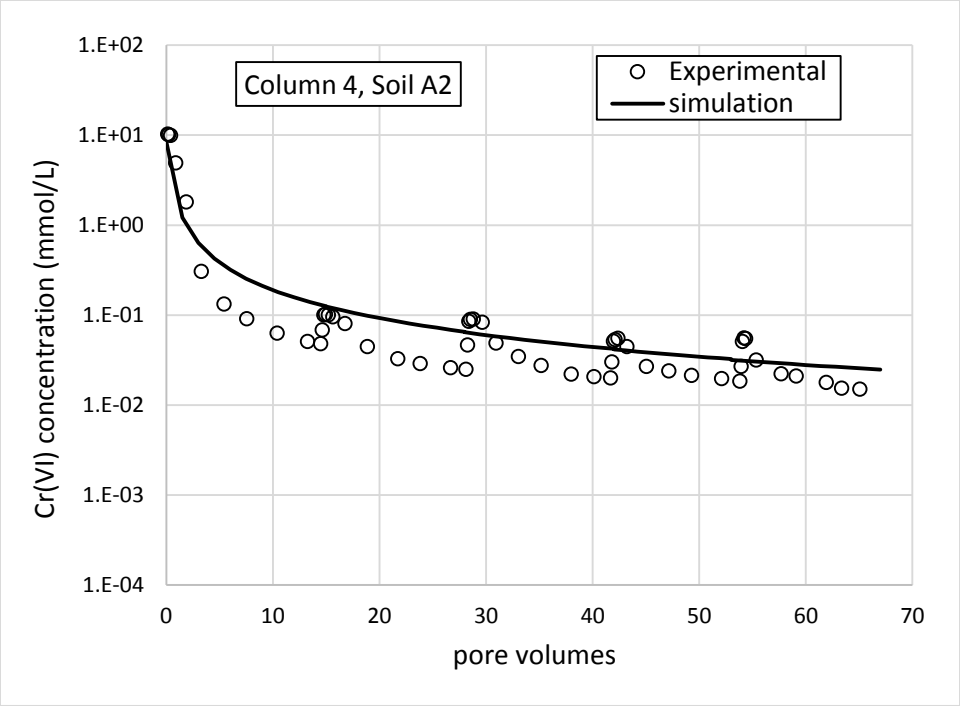

Figure 17. Fitted Cr(VI) Concentrations Using Equilibrium_All Model for Column 4 (Soil A2)

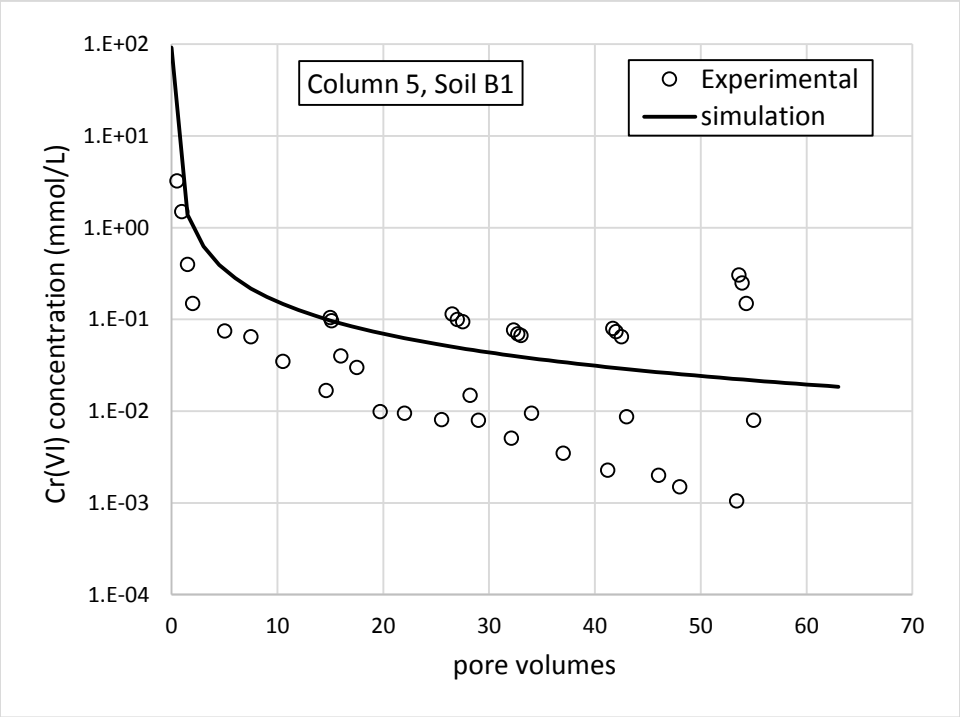

Figure 18. Fitted Cr(VI) Concentrations Using Equilibrium_All Model for Column 5 (Soil B1)

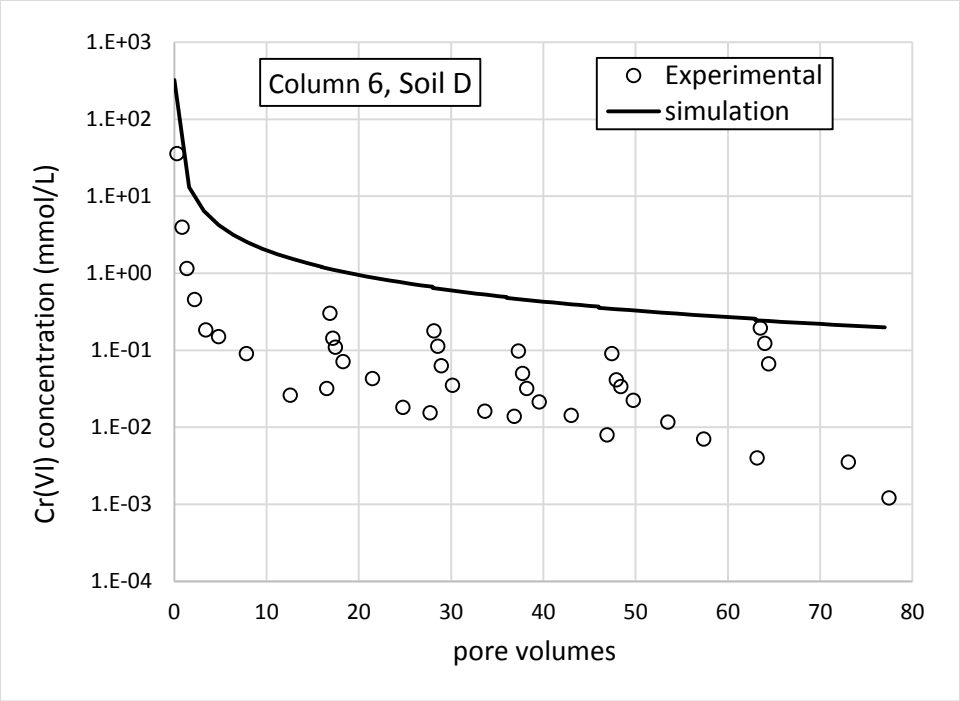

Figure 19. Fitted Cr(VI) Concentrations Using Equilibrium_All Model for Column 6 (Soil D)

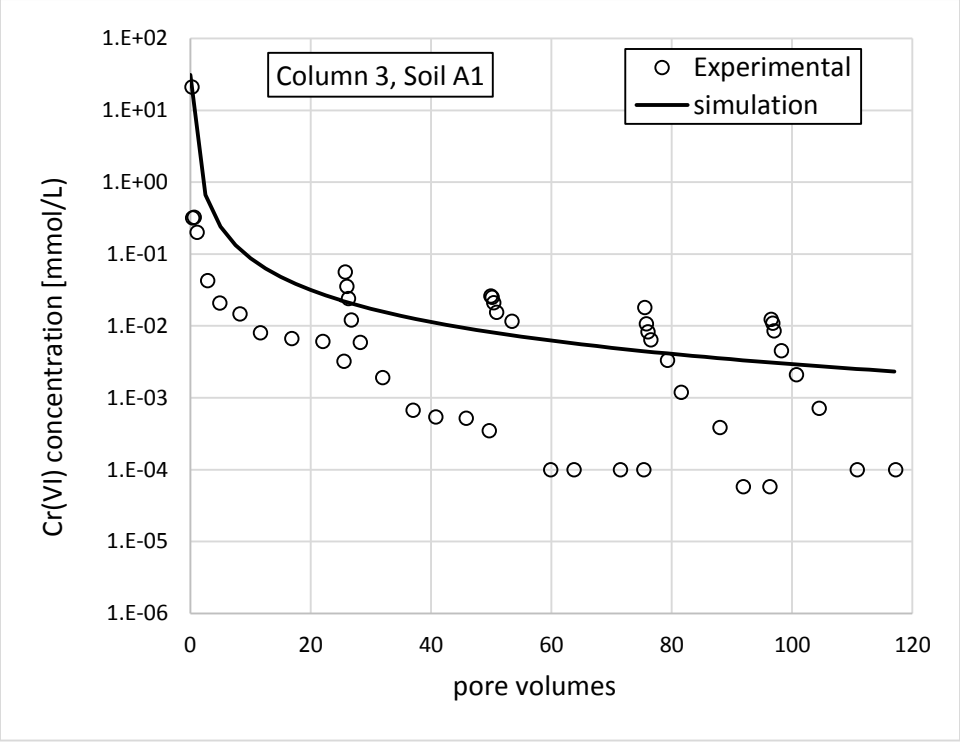

Figure 20. Fitted Cr(VI) Concentrations Using Equilibrium_1stFlow Model for Column 3 (Soil A1)

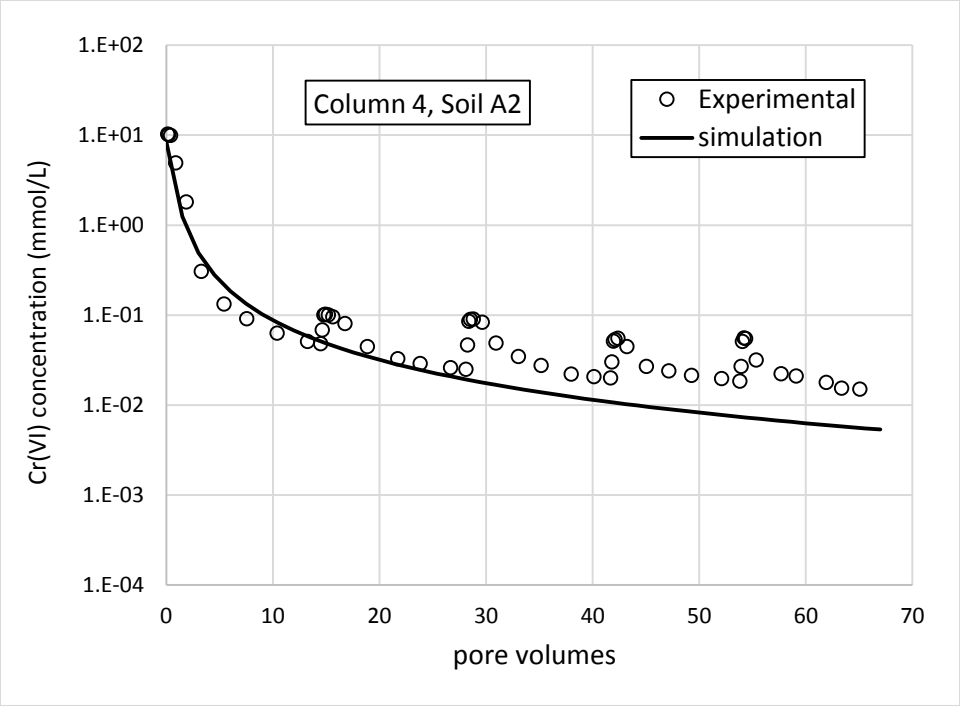

Figure 21. Fitted Cr(VI) Concentrations Using Equilibrium_1stFlow Model for Column 4 (Soil A2)

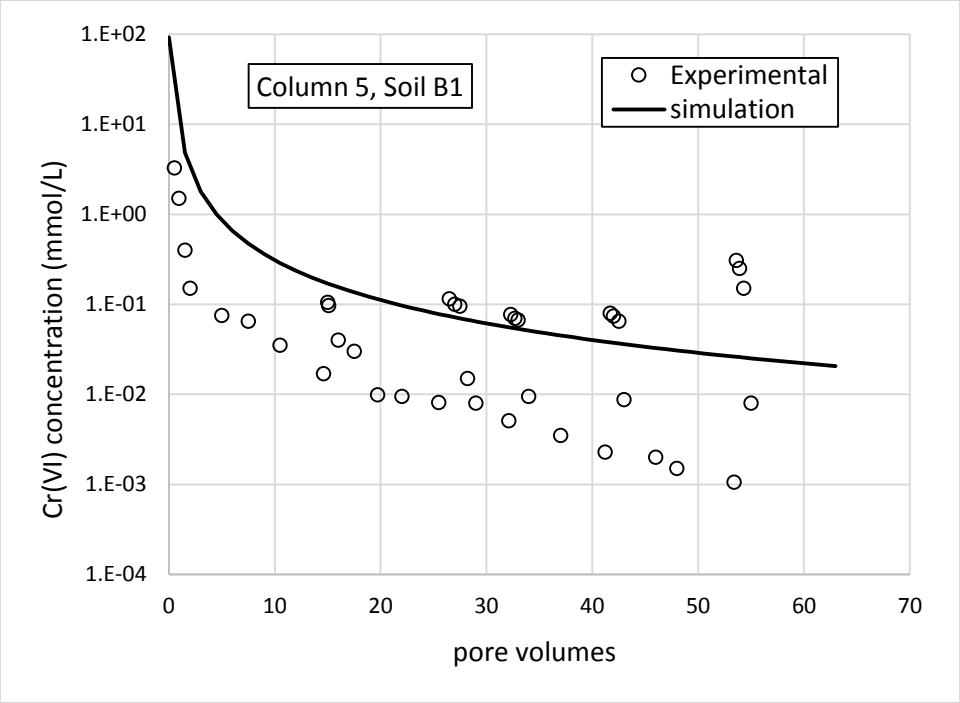

Figure 22. Fitted Cr(VI) Concentrations Using Equilibrium_1stFlow Model for Column 5 (Soil B1)

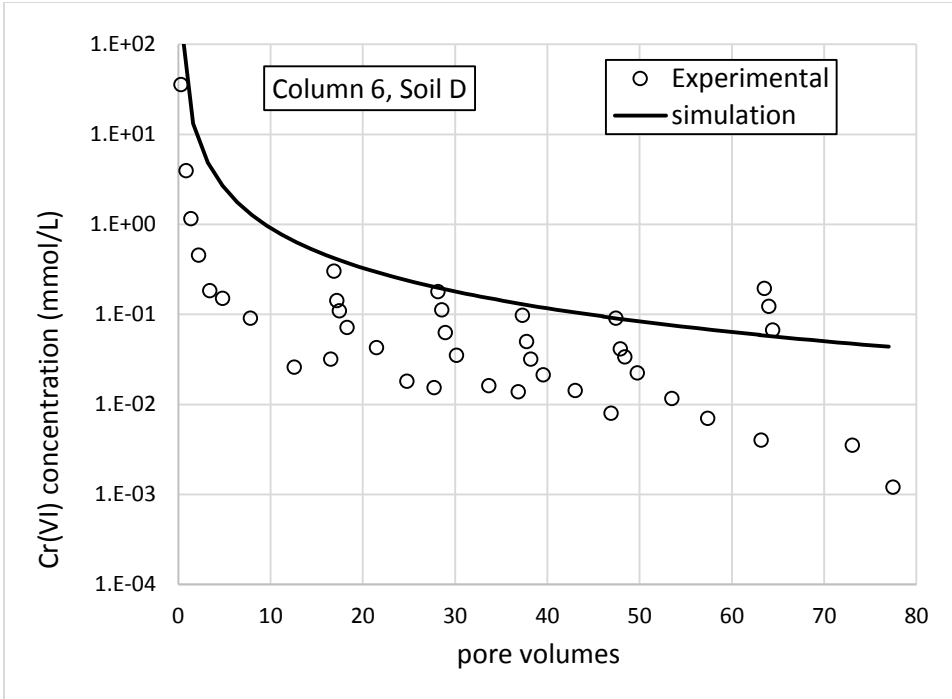

Figure 23. Fitted Cr(VI) Concentrations Using Equilibrium_1stFlow Model for Column 6 (Soil D)

7 Results

A Cr release rate is calculated directly from the experiment data as the difference quotient as shown in Equation 13:

$$release\,rate = \frac{C_{effluent}^{n+1} - C_{effluent}^{n}}{t_{n+1} - t_n} \qquad \text{Equation 13}$$

where n denotes the nth time level. The effluent mass release rate is normalized with respect to the initial solid Cr(VI) concentration (Table 2) and with respect to the Darcy flux to develop release rate parameters that can be applied to any other location based on information related to initial soil concentration and Darcy flux (e.g., recharge rate or average flow within the PRZ). The average Darcy flux for each column experiment is given in Table 1 (in units of cm/hr) and, when converted to units of m/day, results in values of 0.94, 0.56, 0.56, and 0.69 m/day for Columns 3, 4, 5, and 6, respectively. The units of m/day are more appropriate as transport calculations in the 100-BC scale appropriate groundwater flow and transport model are performed using daily and monthly stress periods.

For each column the normalized mass release rates are calculated based on the kinetic sorption model and the equilibrium sorption model (Equilibrium_1st Flow model). These results are presented in Figure 25. The units of the normalized mass release rate are in mg/day of Cr(VI) released per mg/kg of initial Cr(VI) soil concentration per m/day Darcy flux. The results from first five pore volumes are not included because they lead to very high normalized release rates and are not applicable to evaluating long-term release rates. The normalized release rates of interest are those that occur generally greater than 20 pore volumes and reflect the likely long-term release based on desorption rates. The normalized release rates are not calculated under the stop-flow conditions as the Darcy flux is zero resulting in breaks in curves.

Column	Kinetic Sorption Model	Equilibrium_1stFlow Model
3	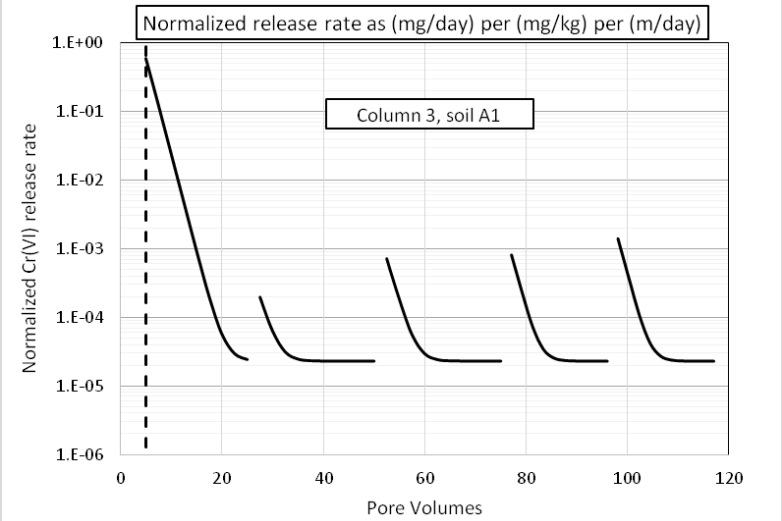	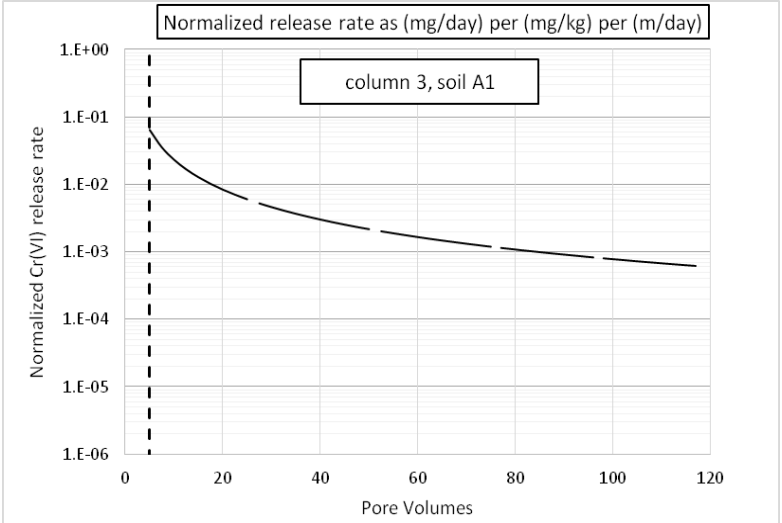
4	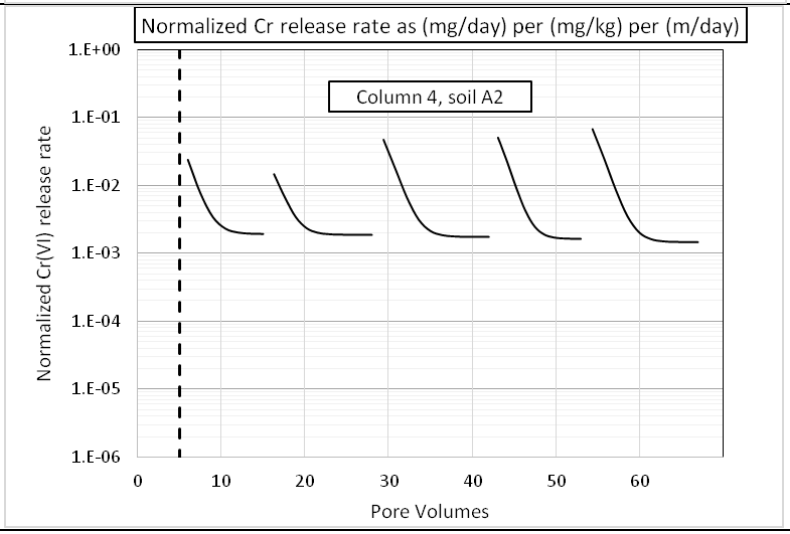	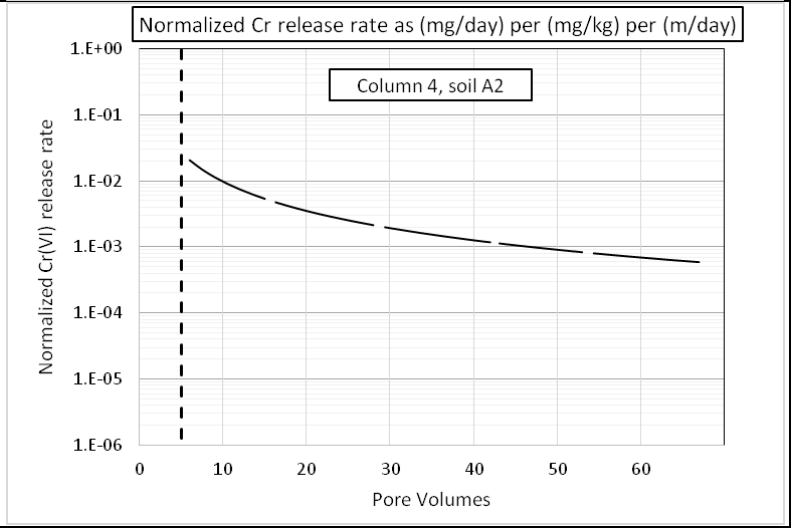

Figure 24. Mass Release Rates of Cr(VI) as a Function of Pore Volumes Based on the Kinetic and Equilibrium Sorption Models Normalized to Initial Soil Concentration and Darcy Flux
(sheet 1 of 2)

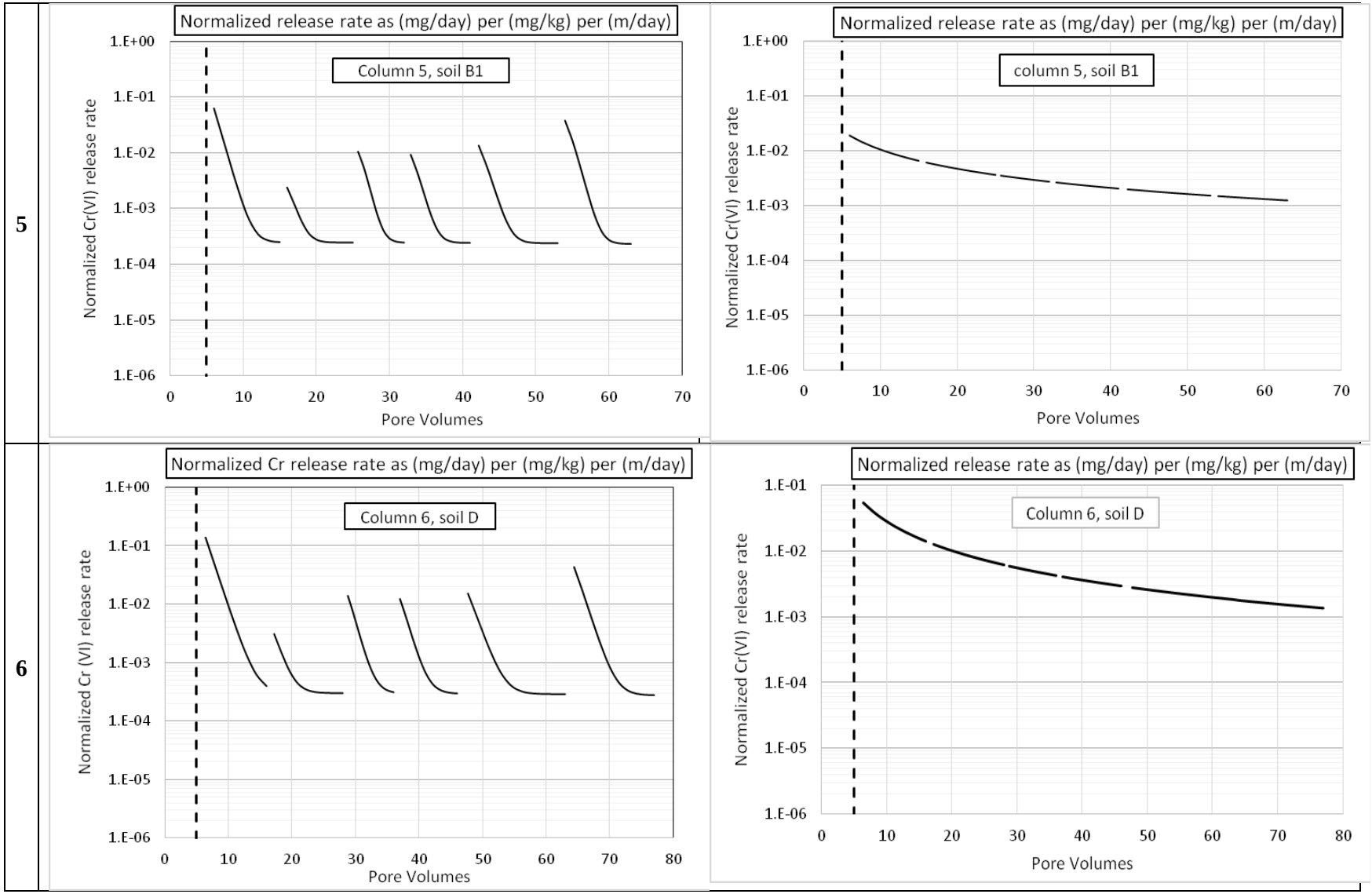

Figure 25. Mass Release Rates of Cr(VI) as a Function of Pore Volumes Based on the Kinetic and Equilibrium Sorption Models Normalized to Initial Soil Concentration and Darcy Flux
(sheet 2 of 2)

The results of the kinetic sorption model are sensitive to the flow conditions and show increased release rates upon the resumption of flow (after the stop-flow event) and reaching an asymptotic low release rate within few pore volumes. The normalized release rates based on the kinetic sorption model range over two orders of magnitude (generally from 10^{-4} to 10^{-2}). These results indicate that sorption sites of varying binding strengths are involved in controlling release along with dissolution of Cr(VI)-bearing mineral phases. Upon resumption of flow the sorption sites where the Cr(VI) ions (such as CrO_4^{2-}) are weakly complexed are released into the pore waters while the sorption sites where Cr(VI) is moderately to strongly complexed (as inner spheres) leach out slowly and control the release under the flowing conditions. The equilibrium sorption model-based normalized release rates do not show any variation at the resumption of flow as the model is based on assumption of establishment of local equilibrium conditions, which only occurs during the stop-flow event. Therefore, the normalized release rates for the equilibrium sorption model are high and match those calculated for the kinetic sorption model at the resumption of flow. However, for Column 4 the normalized release rates of the two models match, indicating that local equilibrium conditions are being established.

Under conditions such as those in aquifers, where persistent flow occurs, the normalized release rates for the purpose of developing a source release function should be taken from the kinetic sorption model when they are near the asymptote values. The recommended normalized release rates are 10^{-3} to 10^{-4} mg/day per mg/kg initial soil concentration per m/day Darcy flux. These reflect the natural variability in release rates due to varying mineral phases that control release of Cr(VI). When the conditions are such that flow is either near stagnant or episodic (e.g., under diffuse recharge conditions within the vadose zone or in the PRZ with intermittent flow due to seasonal rain events or river stage fluctuations), the normalized release rates derived from the stop-flow events are more applicable. As discussed earlier (Figure 7), the normalized Cr(VI) release rates following the 24-hour stop-flow event range from 1×10^{-4} to 6×10^{-4} mg/day per mg/kg initial soil concentration. This range is recommended for evaluating release from the vadose zone and PRZ.

The recommended normalized release rates, however, cannot be directly applied to the bulk soil volume since these release rates are based on conducting experiments in columns where the gravel fraction has been removed. The diameter of the PVC column is about 10.5 cm (Table 1), and therefore typically only the <2 mm sized sediments are packed within the column. For calculating the normalized release rate for the bulk volume a gravel fraction correction is needed. This correction factor can be chosen to be the same as the average gravel fraction in the sediment based on the assumption that almost all reactive sites (sorption site) are associated with the <2 mm sized fraction (e.g., sand, silt, and clay), and no Cr(VI) sorption occurs on the gravel. If the bulk gravel content in the 100-BC Area sediments that are deemed contaminated is about 50%, then the normalized release rates should be multiplied by 0.5. The gravel content within the 100 Area vadose zone sediments is highly variable and for the purpose of performing a gravel correction, a value of 0.5 is recommended.

The long-term predictive modeling of the source term (leaching from contaminated sediments in the vadose zone and PRZ) needs to account for declining release rates as a function of pore volume. The cumulative release fraction presented in Figure 8 indicates that by about 20 pore volumes most of the leachable mass has been released, and any further release usually occurs much more gradually with continuous decline in the release rate (as indicated by the slope of the line). By about 60 pore volumes, it appears that very little Cr(VI) mass can be leached out and the release rate becomes negligibly small, indicating that the Cr(VI)-bearing mineral phase is undergoing very slow dissolution. For all practical purposes the upper limit of leachable Cr(VI) mass appears to be reached by about 60 to 80 pore volumes. In order to quantify the long-term decline in source strength as a function of pore volume, the results presented in Figure 9 were evaluated by excluding all empirically derived K_d values prior to 20 pore volumes. The remaining K_d values (beyond 20 pore volumes) were considered, and a power function fit

was performed on all the data including those from the stop-flow events as shown in Figure 26. The choice of 20 pore volumes is somewhat arbitrary; choosing any other number of pore volumes (beyond 20 pore volumes) will not appreciably change the regression results but would lead to a lower number of data points for estimating the goodness of fit.

Taking the regressed results (regression equation fit line = 15 × [pore volume]$^{0.68}$), where the desorption K_d increases as a function of cumulative pore volume beyond 20 pore volumes, a leach rate adjustment multiplier is calculated as shown in Figure 27. This result is consistent with the observed increase in desorption K_d as a function of pore volume that reflects reducing leachability of the residual Cr(VI) mass with increasing pore volume flushing. The leach rate adjustment multiplier considers that the leach rate at the current time is based on the normalized release rates (as discussed earlier) but then the rate should decline gradually to be consistent with the observations. The leach rate adjustment multiplier reduces the release rate as a function of future pore volumes so that lower mass is released consistent with the observations of a gradually increasing cumulative release fraction presented in Figure 8.

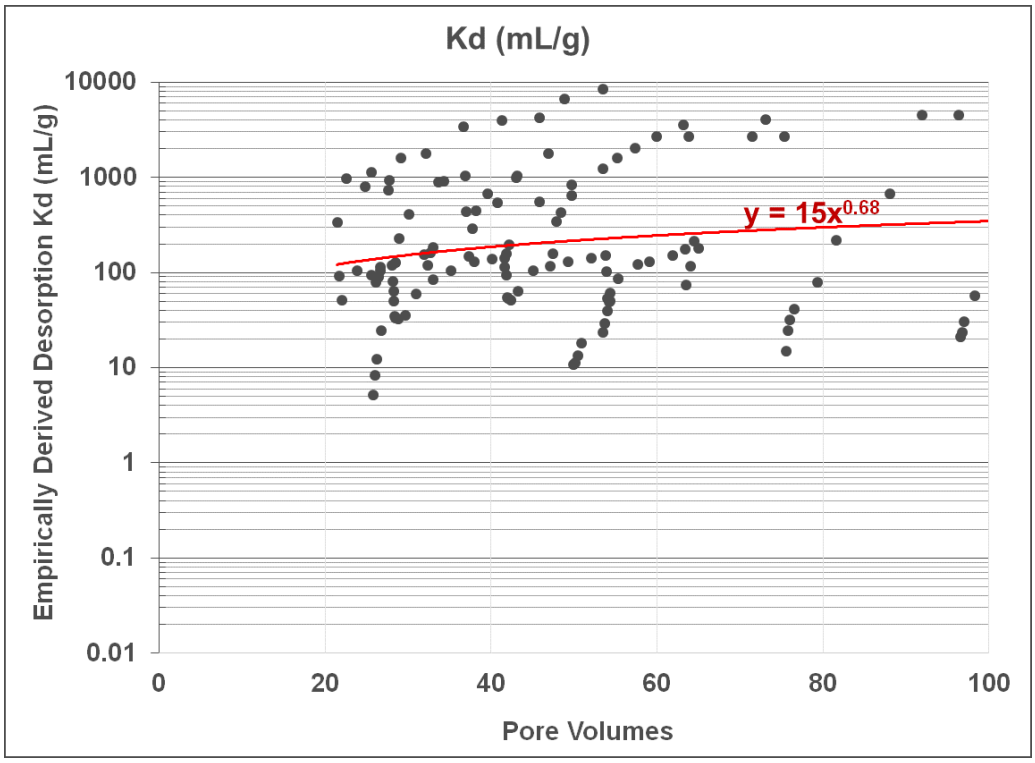

Figure 25. Regression Fit to Empirically Derived Desorption K_d Values Beyond 20 Pore Volumes

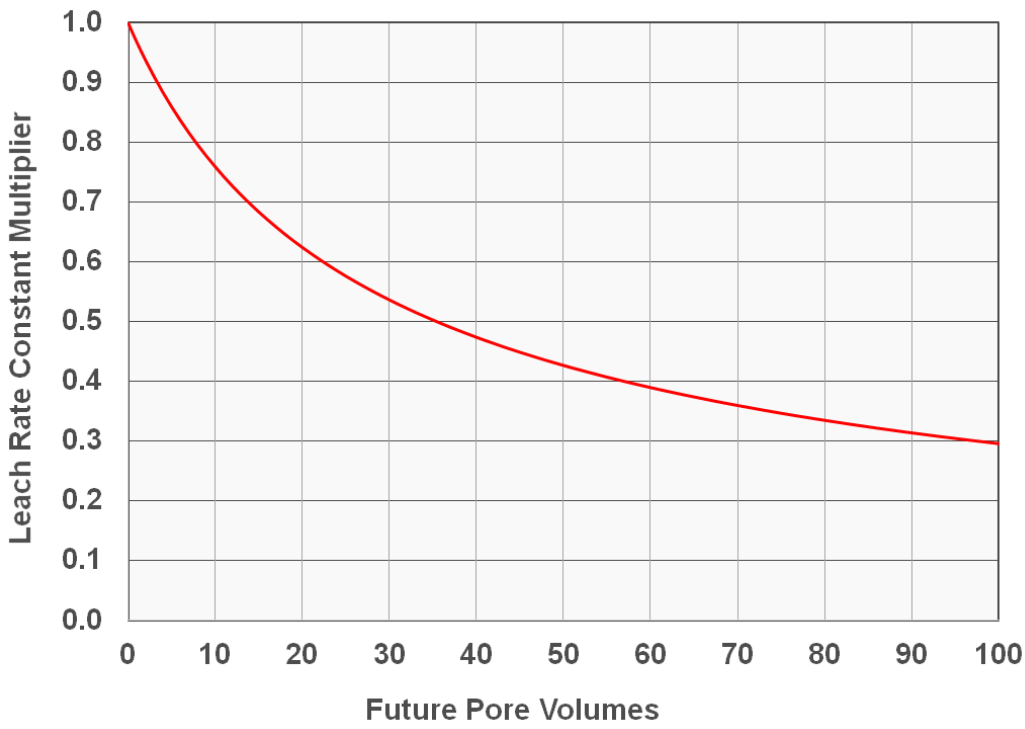

Figure 26. Leach Rate Constant Multiplier to Quantify the Declining Source Strength for Release of Cr(VI)

8 Conclusions

The focus of this study was to evaluate the leaching characteristics of Cr(VI) from the contaminated vadose zone sediments at the 100-BC Area (including the 100-BC-5 Operable Unit and surrounding region) of the Hanford Site and develop transport parameters that can be used in predicting the long-term mass flux of Cr(VI) to the unconfined aquifer from contaminated sediments in the vadose zone and PRZ.

Desorption rates of Cr(VI) were developed based on a single-site kinetic sorption model and an equilibrium sorption model. The desorption rates under stop-flow conditions were also derived. The parameters developed are internally consistent since they are based on the same set of column tests performed on contaminated sediments collected within the 100-BC Area. The Cr(VI) normalized mass release rates developed for the vadose zone and PRZ are based on evaluation of mass release characteristics under stop-flow conditions while the normalized release rates for the aquifer are based on uninterrupted flow conditions. In addition, a leach rate constant multiplier is developed that reduces the leach rate for the predicting the mass release in the future.

9 References

ECF-100BC5-15-0118, 2015, *Initial Chromium Concentration Development to Support Fate and Transport Modeling for Remedial Investigation/Feasibility Study of the 100-BC Operable Units*, CH2M HILL Plateau Remediation Company, Richland, Washington.

PNNL-17674, 2008, *Geochemical Characterization of Chromate Contamination in the 100 Area Vadose Zone at the Hanford Site*, Pacific Northwest National Laboratory, Richland, Washington. Available at: http://www.pnl.gov/main/publications/external/technical_reports/PNNL-17674.pdf.

Qafoku, N.P., P.E. Dresel, J.P. McKinley, C. Liu, S.M. Heald, C.C. Ainsworth, J.L. Phillips, and J.S. Fruchter, 2009, "Pathways of Aqueous Cr(VI) Attenuation in a Slightly Alkaline Oxic Subsurface," *Environmental Science & Technology*, Vol. 43, p. 1071-1077.

This page intentionally left blank.

Appendix A

Finite Difference Approximation

This page intentionally left blank.

A1 Introduction

The mathematical model for solving the mass transport equations listed in Chapter 6 (see Equations 1 and 11 in the main text) is approximated by a finite difference scheme that is described here in more detail.

Consider a finite difference discretization of space and time. Denote the spatial cell discretization indices, i = 1, 2, …, N_z, where N_z is the number of grid cells. The length of each grid cells (Δz) is the column length divided by N_z. Denote the time discretization indices by $n = 0, 1, 2, \ldots, N_t$, where N_t is the number of time steps. The initial conditions provide the concentrations at time $t_0 = 0$. A general time step is from time t_n to time t_{n+1}, where the solution is known at the beginning of the time step, t_n, and is unknown at the end of the time step, t_{n+1}. The change in time over a time step is $\Delta t = t_{n+1} - t_n$. Consider the discretization of Equations 1 and 4 (Chapter 6) at the ith grid cell. The first-order discretization of the time derivatives are, respectively,

$$\frac{\partial C}{\partial t} \approx \frac{C_i^{n+1} - C_i^{n+1}}{t_{n+1} - t_n} \text{ and } \frac{\partial q}{\partial t} \approx \frac{q_i^{n+1} - q_i^{n+1}}{t_{n+1} - t_n}$$

where i is grid cell index and n is time level.

The second order discretization of the dispersive term at the ith grid cell is

$$\frac{\partial^2 C}{\partial z^2} = \frac{C_{i+1} - 2C_i + C_{i-1}}{\Delta z^2}$$

and the first-order upstream weighted discretization of the advective term at the ith grid cell is

$$\frac{\partial C}{\partial z} = \frac{C_i - C_{i-1}}{\Delta z}.$$

The finite difference equation approximation for the Cr transport, Equation 1, is

$$\frac{C_i^{n+1} - C_i^n}{\Delta t} = \theta D \frac{C_{i+1} - 2C_i + C_{i-1}}{\Delta z^2} - v \frac{C_i - C_{i-1}}{\Delta z} - \rho_b \frac{q_i^{n+1} - q_i^n}{\Delta t} \qquad \text{Equation A-1}$$

and for the kinetic sorption, Equation 4, is

$$\frac{q_i^{n+1} - q_i^{n+1}}{\Delta t} = \alpha_r K_d C_i - \alpha_r q_i \qquad \text{Equation A-2}$$

Only the time derivatives in these equations show the time level of the concentrations. If the dispersive, advective, and solid (sorbed) concentration terms are evaluated at the beginning of the time step, t_n, the method is said to be explicit. The explicit method can experience serious numerical instability for some choices of the space/time discretization. For this reason, all the terms in Equations A-1 and A-2 are evaluated at the unknown time level t_{n+1}. These finite difference equations exhibit numerical stability, and the resulting finite difference equations are said to be fully implicit.

Equation A-1 written in tridiagonal form is shown in Equation A-3:

$$-\left(\frac{\theta D}{\Delta z^2}+\frac{v}{\Delta z}\right)C_{i-1}^{n+1}+\left(\frac{2\theta D}{\Delta z^2}+\frac{v}{\Delta z}+\frac{\theta}{\Delta t}\right)C_i^{n+1}-\frac{\theta D}{\Delta z^2}C_{i+1}^{n+1}+\frac{\rho_b}{\Delta t}q_i^{n+1} = \frac{\theta}{\Delta t}C_i^n+\frac{\rho_b}{\Delta t}q_i^n \qquad \text{Equation A-3}$$

and the kinetic sorption equation is shown in Equation A-4

$$-\frac{\alpha_f\theta}{\rho_b}C_i^{n+1}+\left(\frac{1}{\Delta t}+\alpha_r\right)q_i^{n+1}=\frac{q_i^n}{\Delta t} \qquad \text{Equation A-4}$$

This coupled system of linear equations uses known information at the beginning of the time step, C_i^n and q_i^n, to calculate the concentrations C_i^{n+1} and q_i^{n+1}.

At the upper cell a no-flow condition is imposed for both dispersive and advective transport. At the lower boundary there is no dispersive transport. The advective mass transport at the lower boundary of the column, $i = Nz$, is computed as $Q_{inj}\Delta t C_{Nz}^{n+1}$. The effluent concentration reported is the concentration at grid block $i = Nz$.

The mathematical model for equilibrium sorption, Equation 11, uses the same discretization as above, but the partition coefficient is now a function of pore volumes or time. A fully implicit discretization of Equation 11 in tridiagonal form is shown in Equation A-5:

$$-\left(\frac{\theta D}{\Delta z^2}+\frac{v}{\Delta z}\right)C_{i-1}^{n+1}+\left(\frac{\theta}{\Delta t}+\frac{\rho_b K_d^{n+1}}{\Delta t}+\frac{2\theta D}{\Delta z^2}+\frac{v}{\Delta z}\right)C_i^{n+1}-\frac{\theta D}{\Delta z^2}C_{i+1}^{n+1} = \frac{\theta C_i^n}{\Delta t}+\frac{\rho_b K_d^n C_i^n}{\Delta t} \qquad \text{Equation A-5}$$

where the partition coefficient is evaluated at the implicit time level.

Appendix B

MATLAB® Input File for Column 3 Kinetic Sorption Model Calculation

This page intentionally left blank.

B1 Introduction

The model calculations were implemented as MATLAB[1] script using two input files. The two files need to run sequentially by typing each file name from the Matlab command line.

The first file "Transport_Data_Cr.m" is to initiate the necessary model input in Matlab Workspace (i.e., memory). Inputs include the configuration of the column, soil properties, Cr sorption parameters, initial conditions, one-dimensional spatial discretization, preset solution time steps, and the applied experimental flow dynamics. Each script block is explained further in the comment lines (preceded by the % sign).

The second file "Transport_Cr.m" is where the model calculations are implemented and output is exported to Microsoft®[2] Excel®[3]files. The calculation is done at the predefined steps using matrix operations utilizing Matlab's built-in matrix functions. In another nested loop the finite difference equations that were derived in Appendix A are implemented at each prediscretized point of the soil column and are also updated according to initial conditions at the upper and lower ends of the column. This loop results in a coefficient matrix that is consequently inverted to determine the one-dimensional concentration profiles of Cr in water and in solids. Then the time iteration continues to update these concentration profiles at all time steps. Within each time step the evaluated concentrations and designed flows (injected pore volumes) are used to evaluate mass fluxes and check the mass balance.

After the time loop finishes, the predicted concentration profiles and mass balances are stored for each time step; then results are exported to an output Excel file (e.g., "Column_3_Cr_Kinetic.xlsx"). The output Excel file is designed with preset graphs to compare the simulated results against the experimental data. The same run is repeated for each column after adjusting the relevant parameters in the first Matlab script file and designating the right output file in the second Matlab script file. Thus, each column experiment is presented by its preset Matlab script and output Excel files. Similar calculations are performed using the equilibrium sorption model.

1 MATLAB is a registered trademark of The Mathworks, Inc.

2 Microsoft is a registered trademark of Microsoft Corporation in the United States and in other countries.

3 Excel is a registered trademark of Microsoft Corporation in the United States and in other countries.

B.1: MATLAB Input File Used To Match Column 3 Results Using Single-Site Kinetic Sorption Model

File name: Transport_Data_Cr.m

```
%Input data for Chromium kinetic sorption leaching model
%Reference Data: Dresel, et. al., "Geochemical Characterization in the
%100 Area Vadose Zone at the Hanford Site", PNNL-17674
%Reference data includes pore volume, water content, soil bulk density,
%injection rate, Darcy flux, and dispersion coefficient.
%The chromium input data is pre-processed from the reference data.
%units internal to code:
%length[cm]
%time[hr]
%concentration[mmol/cm^3]
%mass[g]
%
%column length[cm]
L = 10.46;
%spatial discretization of column
Nz = 20;
delz = L/Nz;
%cell center location
z    = zeros(Nz,1);
z(1) = 0.5*delz;
for i = 2:Nz
    z(i) = z(i-1) + delz;
end
%diameter of column[cm] and area[cm^2] normal to flow
diameter_column = 2.552;
Az = pi()*(diameter_column/2)^2;
%cell bulk volume[cm^3];
V_bulk = L*Az;
%saturated water content = porosity
wtr_content = 0.377;
%volume of water per unit pore volume
Vwtr_per_PV = wtr_content*V_bulk;
%water injection rate[cm^3/hr]: cm^3/min converted to cm^3/hr
inj_rate = 0.333*60;
%Darch velocity[cm/hr]
v = inj_rate/Az;
%dispersion coefficient[cm^2/hr]
Dispersion = 27.3;
%bulk density[g/cm^3]
bulk_density = 1.68;
%initial solid concentration[PNNL-17674-Table 2.1,Alkaline leach, mg/kg
%convert to mmol/g-solid]
conc_solid_initial = 102.6/52/1000;
%initial dissolved Cr concentration [mg/l] [PNNL-17674-Table 2.3]. Convert
%to mmol/cm^3]. Note for Cr 52mmol/mg.
conc_water_initial = 1612/52/1000;
%sorption coefficient [cm^3-water/g-solid]
K_d    = conc_solid_initial/conc_water_initial;
%reverse reaction rate [1/hr]
rate_r = 1.0E-5;
%forward reaction rate
rate_f = rate_r*K_d*bulk_density/wtr_content;
%initial water and solid mass[g]
initial_mass_water = wtr_content*V_bulk*conc_water_initial;
initial_mass_solid = bulk_density*V_bulk*conc_solid_initial;
%conc_old and conc_solid_old are the water and solid concentrations at
```

```
%the beginning of a time step. At the start of the run they are set to the
%respective initial concentration values.
conc_old       = zeros(Nz,1);
conc_solid_old = zeros(Nz,1);
conc_old       = conc_water_initial*ones(Nz,1);
conc_solid_old = conc_solid_initial*ones(Nz,1);
%initial mass in place is sum of water and solid mass in place
initial_massinplace = initial_mass_water + initial_mass_solid;
%
%data describing stop flow events are from %Reference Data: Dresel, et. al.,
%Geochemical Characterization in the 100 Area Vadose Zone at the Hanford
%Site", PNNL-17674, Figures 3.2. For Column 3 there are 4 stop flow events.
%The length of the stop flow events in hours is given by array SF_time.
%Array stop_flow(hours) provides the length of each stop flow event.
%SF_time provides the length of each stop flow event in hours. The first
%flow event is 0-25 PVs followed by the first stop flow event of 24 hours.
%The second flow event is 25-50 PVs followed by the second stop flow event
%of 96 hours and so on. Note that there is no change in pore volume during
%the stop flow events. Each flow event and stop flow event is discretized
%by 10 time steps. The time step schedule over all flow and stop flow
%events is calculated
stop_flow = zeros(5,1);
stop_flow = [25,50,75,96,117];
SF_time = zeros(4,1);
SF_time = [24,96,96,168];
NT      = 90;
PV      = zeros(NT,1);
t       = zeros(NT,1);
delt    = zeros(NT,1);
FLOW_FLAG = zeros(NT,1);
%first flow event
delpv   = stop_flow(1)/10;
dt      = delpv*wtr_content*V_bulk/inj_rate;
t(1)    = dt;
delt(1) = dt;
PV(1)   = delpv;
FLOW_FLAG(1) = 1;
for i = 2:10
    t(i)         = t(i-1) + dt;
    delt(i)      = dt;
    PV(i)        = PV(i-1) + delpv;
    delt(i)      = dt;
    FLOW_FLAG(i) = 1;
end
%first stop flow event
dt            = SF_time(1)/10;
t(11)         = t(10) + dt;
delt(11)      = dt;
PV(11)        = PV(10);
FLOW_FLAG(11) = 0;
for i = 12:20
    t(i)         = t(i-1) + dt;
    delt(i)      = dt;
    PV(i)        = PV(i-1);
    FLOW_FLAG(i) = 0;
end
%2nd flow event
delpv         = (stop_flow(2) - stop_flow(1))/10;
dt            = delpv*wtr_content*V_bulk/inj_rate;
t(21)         = t(20) + dt;
delt(21)      = dt;
PV(21)        = PV(20) + delpv;
FLOW_FLAG(21) = 1;
```

```
for i = 22:30
    t(i)          = t(i-1) + dt;
    delt(i)       = dt;
    PV(i)         = PV(i-1) + delpv;
    FLOW_FLAG(i) = 1;
end
%2nd stop flow event
dt             = SF_time(2)/10;
t(31)          = t(30) + dt;
delt(31)       = dt;
PV(31)         = PV(30);
FLOW_FLAG(31) = 0;
for i = 32:40
    t(i)          = t(i-1) + dt;
    delt(i)       = dt;
    PV(i)         = PV(i-1);
    FLOW_FLAG(i) = 0;
end
%3rd flow event
delpv          = (stop_flow(3) - stop_flow(2))/10;
dt             = delpv*wtr_content*V_bulk/inj_rate;
t(41)          = t(40) + dt;
delt(41)       = dt;
PV(41)         = PV(40) + delpv;
FLOW_FLAG(41) = 1;
for i = 42:50
    t(i)          = t(i-1) + dt;
    delt(i)       = dt;
    PV(i)         = PV(i-1) + delpv;
    FLOW_FLAG(i) = 1;
end
%3rd stop flow event
dt             = SF_time(3)/10;
t(51)          = t(50) + dt;
delt(51)       = dt;
PV(51)         = PV(50);
FLOW_FLAG(51) = 0;
for i = 52:60
    t(i)          = t(i-1) + dt;
    delt(i)      = dt;
    PV(i)         = PV(i-1);
    FLOW_FLAG(i) = 0;
end
%4rd flow event
delpv          = (stop_flow(4) - stop_flow(3))/10;
dt             = delpv*wtr_content*V_bulk/inj_rate;
t(61)          = t(60) + dt;
delt(61)       = dt;
PV(61)         = PV(60) + delpv;
FLOW_FLAG(61) = 1;
for i = 62:70
    t(i)          = t(i-1) + dt;
    delt(i)       = dt;
    PV(i)         = PV(i-1) + delpv;
    FLOW_FLAG(i) = 1;
end
%4th stop flow event
dt             = SF_time(4)/10;
t(71)          = t(70) + dt;
delt(71)       = dt;
FLOW_FLAG(71) = 0;
PV(71)         = PV(70);
for i = 72:80
```

```
        t(i)         = t(i-1) + dt;
        delt(i)      = dt;
        PV(i)        = PV(i-1);
        FLOW_FLAG(i) = 0;
    end
    %5th flow event
    delpv         = (stop_flow(5) - stop_flow(4))/10;
    dt            = delpv*wtr_content*V_bulk/inj_rate;
    t(81)         = t(80) + dt;
    delt(81)      = dt;
    FLOW_FLAG(81) = 1;
    PV(81)        = PV(80) + delpv;
    for i = 82:90
        t(i)         = t(i-1) + dt;
        delt(i)      = dt;
        PV(i)        = PV(i-1) + delpv;
        FLOW_FLAG(i) = 1;
    end
    %end of time step schedule
    %The input array is assigned the input parameters and is written to the
    %results file from the transport calculation file Transport_Cr.m
    input = zeros(12,1);
    input = [L,diameter_column,Nz,wtr_content,inj_rate,Dispersion,...
             bulk_density,conc_water_initial,conc_solid_initial,...
             K_d,rate_r,rate_f];
    'fini Transport_Data_Cr'
```

B.2: MATLAB Input File Used To Match Column 3 Results Using Single-Site Kinetic Sorption Model File name: Transport_Cr.m

```
%finite difference solution of advective/dispersive transport with
%kinetic sorption
%
clc
%clf
clear
format long
%read initial data
Transport_Data_Cr
%
%initialize arrays
pore_volumes = zeros(NT,1);
vial_conc    = zeros(NT,1);
balance_ke   = zeros(NT,1);
balance_te   = zeros(NT,1);
mass_wtr     = zeros(NT,1);
mass_solid   = zeros(NT,1);
mass_out     = zeros(NT,1);
%set initial time
time = 0;
%There are 2 equations per grid cell. Neq is the total number
%of equations
Neq = 2*Nz;
%start time step loop
for it = 1:NT
%
    solution   = zeros(Neq,1);
    coef       = zeros(Neq,Neq);
    conc       = zeros(Nz,1);
    conc_solid = zeros(Nz,1);
    time = t(i);
%test for stop flow period
    if FLOW_FLAG(it) == 0
        v = 0;
    else
        v = inj_rate/Az;
    end
%For the ith cell the first equation (index 2*i-1) is the transport mass
%balance equation. The second equation (index 2i) is the kinetic
%sorption equation. In the 1st cell (i=1) the boundary condition is no
%dispersive or advective flux across the boundary. In the last cell (i=Nz)
%there is no dispersive flux out.
%The effluent mass flux out = injection-rate*time-step-size*liquid-
%concentration in the bottom cell (i=Nz).
%The effluent concentration out is the concentration in the bottom cell.
%The coefficient matrix is the coefficients of the unknowns (liquid and
%solid concentrations) in the transport and kinetic sorption equations.
%Generate the coefficient matrix
    coef   = zeros(Neq,Neq);
%loop over grid cells
    for i = 1:Nz
        if i == 1
            coef(2*i-1,2*i-1) = wtr_content*Dispersion/delz/delz + v/delz ...
                                + wtr_content/delt(it);
            coef(2*i-1,2*i+1) = - wtr_content*Dispersion/delz/delz;
            coef(2*i-1,2*i)   = bulk_density/delt(it);
            coef(2*i,2*i)     = 1/delt(it) + rate_r;
            coef(2*i,2*i-1)   = -rate_f*wtr_content/bulk_density;
        elseif i == Nz
            coef(2*i-1,2*i-3) = -(wtr_content*Dispersion/delz/delz + v/delz);
```

```
                coef(2*i-1,2*i-1) = wtr_content*Dispersion/delz/delz + v/delz ...
                                    + wtr_content/delt(it);
                coef(2*i-1,2*i)   = bulk_density/delt(it);
                coef(2*i,2*i)     = 1/delt(it) + rate_r;
                coef(2*i,2*i-1)   = -rate_f*wtr_content/bulk_density;
            else
                coef(2*i-1,2*i-3) = -(wtr_content*Dispersion/delz/delz + v/delz);
                coef(2*i-1,2*i-1) = 2*wtr_content*Dispersion/delz/delz...
                                    + v/delz + wtr_content/delt(it);
                coef(2*i-1,2*i+1) = - wtr_content*Dispersion/delz/delz;
                coef(2*i-1,2*i)   = bulk_density/delt(it);
                coef(2*i,2*i)     = 1/delt(it) + rate_r;
                coef(2*i,2*i-1)   = -rate_f*wtr_content/bulk_density;
            end
        end
    %compute inverse of coefficient matrix
        A_inv = zeros(Neq,Neq);
        A_inv = inv(coef);
    %Assign right hand side vector. This includes terms of the finite
    %difference equations involving known concentrations at the beginning of
    %the time step (*_old).
        rhs = zeros(Neq,1);
        for i = 1:Nz
            rhs(2*i-1) = wtr_content*conc_old(i)/delt(it)...
                         + bulk_density*conc_solid_old(i)/delt(it);
            rhs(2*i)   = conc_solid_old(i)/delt(it);
        end
    %solution for liquid(conc) and solid(conc_solid) concentrations
        solution = A_inv*rhs;
        for i = 1:Nz
            conc(i)       = solution(2*i-1);
            conc_solid(i) = solution(2*i);
        end
    %cumulative mass out
        if it == 1
            mass_out(it) = v*delt(it)*Az*conc(Nz);
        else
            mass_out(it) = mass_out(it-1) + v*delt(it)*Az*conc(Nz);
        end
    %mass balance kinetic equation and transport equation
        balance_ke(it) = 0;
        balance_te(it) = 0;
        mass_wtr(it)   = 0;
        mass_solid(it) = 0;
        for i = 1:Nz;
            mass_ke = bulk_density*(conc_solid(i)-conc_solid_old(i))/delt(it)...
                - rate_f*wtr_content*conc(i)...
                + rate_r*bulk_density*conc_solid(i);
            if i == 1
              mass_te = (wtr_content/delt(it))*(conc(i)-conc_old(i))...
                - (wtr_content*Dispersion/delz/delz)*(conc(i+1)-conc(i))...
                + (v/delz)*conc(i)...
                + (bulk_density/delt(it))*(conc_solid(i)-conc_solid_old(i));
            elseif i == Nz
              mass_te = (wtr_content/delt(it))*(conc(i)-conc_old(i))...
                - (wtr_content*Dispersion/delz/delz)*(conc(i-1)-conc(i))...
                + (v/delz)*(conc(i)-conc(i-1))...
                + (bulk_density/delt(it))*(conc_solid(i)-conc_solid_old(i));
            else
              mass_te = (wtr_content/delt(it))*(conc(i)-conc_old(i))...
                - (wtr_content*Dispersion/delz/delz)*(conc(i-1)-2*conc(i)+conc(i+1))...
                + (v/delz)*(conc(i) - conc(i-1))...
                + (bulk_density/delt(it))*(conc_solid(i)-conc_solid_old(i));
```

```
            end
            if abs(mass_ke) > balance_ke(it)
                balance_ke(it) = abs(mass_ke);
            end
            if abs(mass_te) > balance_te(it);
                balance_te(it) = abs(mass_te);
            end
    %mass in place
            mass_wtr(it)   = mass_wtr(it) + delz*Az*wtr_content*conc(i);
            mass_solid(it) = mass_solid(it)...
                            + delz*Az*bulk_density*conc_solid(i);
        end
    %
    %end loop over grid cells
    %update conc_old
        conc_old       = conc;
        conc_solid_old = conc_solid;
    %number of cumulative pore volumes at time t(it)
        if (it) == 1
            pore_volumes(it) = v*Az*delt(it)/Vwtr_per_PV;
        else
            pore_volumes(it) = pore_volumes(it-1) + v*Az*delt(it)/Vwtr_per_PV;
        end
    %vial or effluent concentration mmol/cm^3 convert to mmol/L
        vial_conc(it) = 1000*conc(Nz);
    %
    %end of time step loop
    end
    %write input information to results file
    xlswrite('Column_3_Cr_Kinetic.xlsx',transpose(input),'Input','B2')
    %write time history of pore volumes and concentration
    xlswrite('Column_3_Cr_Kinetic.xlsx',0,'Column_3_Cr','C4')
    xlswrite('Column_3_Cr_Kinetic.xlsx',0,'Column_3_Cr','D4')
    xlswrite('Column_3_Cr_Kinetic.xlsx',1000*conc_water_initial,'Column_3_Cr','E4')
    xlswrite('Column_3_Cr_Kinetic.xlsx',t,'Column_3_Cr','C5:C94')
    xlswrite('Column_3_Cr_Kinetic.xlsx',pore_volumes,'Column_3_Cr','D5:D94')
    xlswrite('Column_3_Cr_Kinetic.xlsx',vial_conc,'Column_3_Cr','E5:E94')
    %write time history results of mass balance equations
    xlswrite('Column_3_Cr_Kinetic.xlsx',t,'balance','B4:B93')
    xlswrite('Column_3_Cr_Kinetic.xlsx',balance_ke,'balance','C4:C93')
    xlswrite('Column_3_Cr_Kinetic.xlsx',balance_te,'balance','D4:D93')
    %write time history of mass-Cr in liquid and solid phases and effluent
    %mass out
    xlswrite('Column_3_Cr_Kinetic.xlsx',initial_mass_water,'balance','F3')
    xlswrite('Column_3_Cr_Kinetic.xlsx',initial_mass_solid,'balance','G3')
    xlswrite('Column_3_Cr_Kinetic.xlsx',mass_wtr,'balance','F4:F93')
    xlswrite('Column_3_Cr_Kinetic.xlsx',mass_solid,'balance','G4:G93')
    xlswrite('Column_3_Cr_Kinetic.xlsx',mass_out,'balance','H4:H93')
    %
    delete('*.tmp')
    'fini Transport_Cr'
```